Lysophosphatidylcholine acyltransferase 1 is downregulated by hepatitis C virus: impact on production of lipo-viro-particles

Frauke Beilstein, Matthieu Lemasson, Véronique Pène, Dominique Rainteau, Sylvie Demignot, Arielle R Rosenberg

Lysophosphatidylcholine acyltransferase 1 is downregulated by hepatitis C virus: impact on production of lipo-viro-particles

Frauke Beilstein[1,2,†], Matthieu Lemasson[3,†], Véronique Pène[3], Dominique Rainteau[4], Sylvie Demignot[1,2,‡], Arielle R. Rosenberg[3,5,‡]

† or ‡: These authors contributed equally to this work.

[1] Sorbonne Universités, UPMC Univ. Paris 06, Inserm, Université Paris Descartes, Sorbonne Paris Cité, UMR_S 1138, Centre de recherche des Cordeliers, F-75006, Paris, France

[2] EPHE, Ecole Pratique des Hautes Etudes, PSL Research University, Laboratoire de Pharmacologie Cellulaire et Moléculaire, F-75006, Paris, France

[3] Université Paris Descartes, EA 4474 « Hepatitis C Virology», F-75014, Paris, France

[4] UPMC Univ. Paris 06, ERL INSERM U 1157/UMR 7203, F-75012, Paris, France

[5] AP-HP, Groupe Hospitalier Cochin, Service de Virologie, F-75014, Paris, France

Correspondence to

- Sylvie Demignot

Postal address:

UMR_S1138, Centre de Recherche des Cordeliers,

15 Rue de l'Ecole de Médecine,

75006 Paris, France

Telephone number: +33(0)144272411

Fax number: +33(0)143251615

E-mail address: sylvie.demignot@crc.jussieu.fr

- Arielle R. Rosenberg

Postal address:

EA 4474 « Hepatitis C Virology »,

Institut Cochin, Bâtiment Méchain, 2e étage,

22 Rue Méchain,

75014 Paris, France

Telephone number: +33(0)140516493

Fax number: +33(0)140516454

E-mail address: arielle.rosenberg@parisdescartes.fr

Keywords hepatitis C virus morphogenesis; HCV-related steatosis; lipo-viro-particle; primary human hepatocyte; very low density lipoprotein.

List of abbreviations Apo, apolipoprotein; BSA, bovine serum albumin; ffu, focus-forming units; HCV, hepatitis C virus; LD, lipid droplet; LPCAT, lysophosphatidylcholine acyltransferase; LVP, lipo-viro-particle; PHH, primary human hepatocytes; PL, phospholipid; RT-qPCR, quantitative reverse-transcription real-time polymerase chain reaction; TAG, triacylglycerol; SEM, standard error of the mean; VLDL, very-low-density-lipoprotein.

Electronic word count (excluding title page, abstract, references, figures and tables) 3999 words

ABSTRACT

Objective Hepatitis C virus (HCV) is intimately linked with the liver lipid metabolism, devoted to the efflux of triacylglycerols stored in lipid droplets (LDs) in the form of triacylglycerol-rich very-low-density lipoproteins (VLDL): (i) the most infectious HCV particles are those of lowest density due to association with triacylglycerol-rich lipoproteins; (ii) HCV-infected patients frequently develop hepatic steatosis (increased triacylglycerol storage). The recent identification of lysophosphatidylcholine acyltransferase 1 (LPCAT1) as an LD phospholipid-remodelling enzyme prompted us to investigate its role in liver lipid metabolism and HCV infectious cycle.

Design Huh-7.5.1 cells and primary human hepatocytes (PHH) were infected with JFH1-HCV. LPCAT1 depletion was achieved by RNA interference. Cells were monitored for LPCAT1 expression, lipid metabolism and HCV production and infectivity. The density of viral particles was assessed by isopycnic ultracentrifugation.

Results Upon HCV infection, both Huh-7.5.1 cells and PHH had decreased levels of LPCAT1 transcript and protein, consistent with transcriptional downregulation. LPCAT1 depletion in either naïve or infected Huh-7.5.1 cells resulted in altered lipid metabolism characterized by LD remodelling, increased triacylglycerol storage and increased secretion of VLDL. In infected Huh-7.5.1 cells or PHH, LPCAT1 depletion increased production of the viral particles of lowest density and highest infectivity.

Conclusion We have identified LPCAT1 as a modulator of liver lipid metabolism downregulated by HCV, which appears as a viral strategy to increase the triacylglycerol content and hence infectivity of viral particles. Targeting this metabolic pathway may represent an attractive therapeutic approach to reduce both the viral titre and hepatic steatosis.

SIGNIFICANCE OF THIS STUDY

What is already known on this subject?

- The most infectious HCV particles circulate as hybrid lipo-viro-particles (LVPs) consisting of viral and very-low-density lipoprotein (VLDL) components.
- The human hepatocyte is both the cell specialized in the biogenesis of VLDLs and the primary replication site of HCV, but whether the VLDL pathway is usurped for LVP morphogenesis is still a matter of debate.
- Besides the existence of LVPs another clinical feature that links HCV infection with the host lipid metabolism is the high prevalence of liver steatosis, but whether these facts are related is unknown.

What are the new findings?

- Lysophosphatidylcholine acyltransferase 1 (LPCAT1) is identified as a modulator of the liver lipid homeostasis downregulated by HCV.
- LPCAT1 depletion increases LVP production, supporting the idea that HCV indeed hijacks the hepatocellular lipid metabolism for the benefit of highly infectious LVP morphogenesis.
- LPCAT1 depletion also increases VLDL secretion, suggesting that at least some of the mechanisms of LVP morphogenesis and VLDL biogenesis are shared.
- LPCAT1 depletion also causes steatosis, illustrating a possible link between LVP morphogenesis and liver steatosis.

How might it impact on clinical practice in the foreseeable future?

- Our findings designate the LPCAT1-regulated lipid metabolism pathway as an attractive host target for antiviral therapy in most difficult-to-treat patients.
- Compared to other lipid-modulating antiviral approaches expected to aggravate liver steatosis, targeting the LPCAT1-regulated pathway would reduce liver steatosis besides reducing HCV infectious titre.

INTRODUCTION

The hepatitis C virus (HCV) is a leading cause of chronic liver disease worldwide. Unique to this human hepatotropic virus is its tight link with the host lipid metabolism.[1-3] Clinical evidence in chronically infected patients has long recognized the high prevalence of liver steatosis, defined as an accumulation of lipids, essentially accounted for by triacylglycerols (TAGs), in cytosolic lipid droplets (LDs) of hepatocytes. Moreover, HCV particles are heterogeneous in the circulating blood of patients and the most infectious viral particles are those of exceptionally low buoyant density due to their association with apolipoprotein (Apo) B-containing TAG-rich lipoproteins in original structures referred to as lipo-viro-particles (LVPs).[4 5] As hepatocytes are specialized in the assembly and secretion of the ApoB-containing TAG-rich lipoproteins known as very-low-density lipoproteins (VLDLs), a working hypothesis is that LVPs are formed originally within infected cells, the hepatocellular lipid metabolism being hijacked by HCV for the benefit of their morphogenesis.[6-8]

LDs consist of a core of TAGs and cholesterol esters surrounded by a monolayer of phospholipids (PLs) and cholesterol.[9] Importantly, TAGs stored in cytosolic LDs of hepatocytes provide most of the TAGs present in VLDLs through a mechanism of hydrolysis-reesterification.[10 11] Many proteins interact with the LD surface, as shown by proteomic characterization of LDs isolated from hepatic cells.[12 13] The LD proteome includes structural proteins, perilipins, and proteins that control several cellular pathways including lipid metabolism (e.g., lipases, acyltransferases), membrane trafficking, signalling, etc.[14 15] The interaction of these proteins with the LD surface can be modulated through mechanisms, probably of multiple causes, that are only just starting to be clarified.[16 17] Because of the large variety of PLs conferring different physicochemical properties to the LD surface, the nature of

PLs is a factor that can modulate the strength of protein association.[18 19] The most abundant PL of the LD surface is phosphatidylcholine.[20] The lysophosphatidylcholine acyltransferase (LPCAT) family consists of PL-remodelling enzymes[21], among which LPCAT1 and LPCAT2 localise partially to the LD surface where they can synthesize phosphatidylcholine.[22] Moreover, LPCAT1 and LPCAT3, both expressed in hepatocytes, were recently reported to influence lipoprotein secretion from these cells.[23 24]

These considerations prompted us to examine the hypothesis of a potential hijacking of LPCAT-mediated metabolism by HCV. Indeed, LPCAT1 is shown here to be downregulated by HCV. LPCAT1 depletion, in turn, was found to increase the virus infectivity.

MATERIALS AND METHODS

Cell culture, infection and gene silencing

Huh-7.5.1 cells and primary human hepatocytes (PHH) were inoculated with JFH1-HCV at a multiplicity of infection of 0.2 and 2 focus-forming units (ffu)/cell, respectively, as described previously.[25 26] Further details for infection and for transfection with HCV subgenomic replicon or core-encoding plasmid are given in the supplementary material. ShRNA- and siRNA-mediated gene silencing was used to achieve LPCAT1 depletion in Huh-7.5.1 cells and PHH, respectively (see supplementary material).

Gene expression and virological analyses

For details of quantitative reverse-transcription real-time polymerase chain reaction (RT-qPCR), western blotting, confocal microscopy, Apo quantification, and virological analyses,[25-27] see the supplementary material. All analyses were done at day 3 post-

inoculation except for the quantification of negative-strand HCV RNA, which was done at day 1 post-inoculation. Indeed, at later time points multiple rounds of infection are expected to cause a bias in the assessment of viral genome replication per se if production of viral particles is affected.

Lipid analyses

The TAG mass was quantified using the PAP150TG kit (BioMérieux) as described in the supplementary material. For analysis of lipid secretion capacity, cells were incubated for the last 24 h of culture with oleic acid (0.6 mM) in complex with bovine serum albumin (oleic acid/BSA) containing 1 μCi/ml [1-^{14}C] oleic acid, then lipids were extracted from cells and media and fractionated by thin layer chromatography followed by quantification of radioactivity as described previously[28] and in the supplementary material.

Statistical analyses

Results were expressed as the mean ± standard error of the mean (SEM) of at least three independent experiments. Statistical significance was evaluated using Student's *t* test for unpaired two-sided data (* for $p < 0.05$, ** for $p < 0.01$ and *** for $p < 0.001$) after a Shapiro-Wilk test was done to confirm that all data follow a normal distribution.

RESULTS

LPCAT1 is downregulated by HCV

As a starting point we investigated whether HCV infection affects the expression of any member of the LPCAT family in Huh-7.5.1 cells (supplementary figure S1). Only LPCAT1 showed significantly reduced mRNA amounts upon JFH1-HCV inoculation (0.47 ± 0.05),

correlating with reduced LPCAT1 protein amounts as assessed by western blot analysis (0.61 ± 0.09) (figure 1A). Most importantly, confocal microscopy analysis confirmed that at the single-cell level, those cells that were actually infected upon HCV inoculation showed a clear decrease in LPCAT1 signal intensity compared to non-infected cells (figure 1B). We concluded that HCV infection induces downregulation of LPCAT1 expression occurring at least partly at the transcriptional level.

As approaches to unravelling mechanisms of HCV-induced downregulation of LPCAT1, we transfected Huh-7.5.1 cells with either a subgenomic JFH1-HCV replicon or a plasmid encoding JFH1-HCV core protein (figure 2). LPCAT1 expression was unchanged in cells harbouring the subgenomic replicon, suggesting that the downregulation observed upon HCV infection involves neither the virus non-structural proteins nor the viral genome replication step (figure 2A-B). By contrast, cells transfected with core-encoding plasmid had significantly reduced LPCAT1 mRNA amounts at the population level (figure 2C), and most strikingly at the single-cell level those cells that actually expressed HCV core protein had reduced LPCAT1 protein signal intensity (figure 2D). Thus, the sole expression of core protein was sufficient to recapitulate HCV infection-induced downregulation of LPCAT1.

LPCAT1 depletion increases production of HCV particles with high infectivity and low density

Next we wanted to determine whether LPCAT1 downregulation has an impact on HCV infectious cycle. To address this question, we used a lentiviral vector encoding shRNA against LPCAT1 (shLPCAT1). In Huh-7.5.1 cells, this indeed resulted in a strong decrease of LPCAT1 protein and mRNA amounts (0.34 ± 0.1 for both) compared to control cells treated with lentivirus encoding shRNA against luciferase (shLuc) (supplementary figure S2A-B). This depletion was specific to LPCAT1, as the mRNA amount of LPCAT3, the main LPCAT

in hepatocytes,[29] remained unchanged (supplementary figure S2C). An even stronger decrease of LPCAT1 protein and mRNA amounts was observed in shLPCAT1-transduced Huh-7.5.1 cells that were inoculated with HCV (0.17 ± 0.07 and 0.20 ± 0.04, respectively), suggesting an additive effect of HCV infection and shLPCAT1 on LPCAT1 depletion (supplementary figure S2D-E). We also verified that shLPCAT1 transduction had no cytotoxic effect (supplementary figure S3A).

To examine the impact of LPCAT1 depletion on HCV infectious cycle, we first used an infectivity assay to evaluate the production of infectious virus in the culture supernatant. The infectivity titre was significantly increased in LPCAT1-depleted Huh-7.5.1 cells (5.84 ± 2.08) (figure 3A). However, this effect could not be attributed to increased replication of viral genome because upon LPCAT1 depletion the amount of negative-strand HCV RNA was modified neither in these HCV-infected cells (figure 3A) nor in cells harbouring a subgenomic HCV replicon (supplementary figure S4). These results pointed to viral morphogenesis as the step of HCV infectious cycle affected by LPCAT1 depletion. Nevertheless, LPCAT1 depletion had only a slight, not significant tendency to increase the viral load, which reflects the production of physical viral particles irrespective of their infectivity. Accordingly, the specific infectivity (ratio of infectivity titre to viral load) was significantly increased in LPCAT1-depleted cells (3.83 ± 1.69). To exclude putative off-target effects of shLPCAT1, we transfected shLPCAT1-transduced Huh-7.5.1 cells with expression plasmids carrying wild-type or an shLPCAT1-resistant version of LPCAT1 gene (supplementary figure S5A), which led to increasing restoration of LPCAT1 protein expression (supplementary figure S5B). This indeed restrained the shLPCAT1-induced gain in both infectivity titre and specific infectivity in a dose-dependent manner (supplementary figure S5C), with a good linear inverse relationship between LPCAT1 protein amount and

HCV infectivity titre (supplementary figure S5D). Collectively, the data suggested that LPCAT1 depletion favours the morphogenesis of highly infectious virus.

Finally, because HCV infectivity is inversely correlated with the buoyant density of viral particles,[25 30] we subjected culture supernatants from HCV-infected Huh-7.5.1 cells depleted or not for LPCAT1 to isopycnic ultracentrifugation through iodixanol gradients (see a representative experiment in figure 3B-E). As previously reported for HCV grown in Huh-7 cell line,[25 30] the majority of viral RNA peaked between 1.09 and 1.14 g/ml (figure 3B). However, LPCAT1 depletion led to a shift of HCV RNA towards fractions of lower buoyant density: the percentage of total viral load present below 1.08 g/ml was 22.60 ± 1.65% for LPCAT1-depleted cells as compared to 12.59 ± 1.99% for control cells. The excess of highly infectious particles produced upon LPCAT1 depletion was also found in these fractions of lower density (figure 3C). We concluded that LPCAT1 depletion increases the production of HCV particles of high specific infectivity coinciding with low buoyant density.

LPCAT1 depletion leads to LD remodelling, increased TAG storage and increased secretion of TAG-rich lipoproteins

The lower buoyant density of HCV produced upon LPCAT1 depletion was consistent with a TAG enrichment of viral particles, prompting us to examine the impact of LPCAT1 depletion on the hepatocellular lipid metabolism. Confocal microscopy of Huh-7.5.1 cells labelled with BODIPY 493/503 did not show any gross modification of the intracellular LD distribution upon LPCAT1 depletion (figure 4A). However, the mean number of LDs was significantly reduced in LPCAT1-depleted cells compared to control cells (153.20 ± 37.89 and 352.12 ± 78.14 LDs/cell, respectively) (figure 4B). Furthermore, measurement of LD size showed a shift of the LD diameter distribution towards larger LDs upon LPCAT1 depletion (figure 4C). Besides these modifications that might reflect fusion of small LDs into larger ones, the net

intracellular TAG amount was increased in the steady state in LPCAT1-depleted cells (1.72 ± 0.07) (figure 4D). Because hepatic cells produce TAG-rich lipoproteins, this increased intracellular TAG content could result from inhibition of their secretion. Unexpectedly, however, the amount of ApoB, the constitutive apolipoprotein of TAG-rich lipoproteins, was increased in the culture supernatant of LPCAT1-depleted compared to control cells (423.28 ± 84.19 and 175.77 ± 34.35 μg/dl, respectively) (figure 4E), indicating the secretion of a greater number of lipoprotein particles. An impaired capacity to enrich lipoproteins with TAGs could also lead to an increased intracellular TAG content. To test this hypothesis, Huh-7.5.1 cells were challenged with oleic acid containing [1-^{14}C] oleic acid as a tracer then radiolabelled PLs and TAGs were quantified in cells and media (figure 5). The intracellular amounts of newly synthesized PLs and TAGs were similar in LPCAT1-depleted and control cells, indicating similar uptake and lipid synthesis capacity. However, the secretion of newly synthesized TAGs was significantly, albeit slightly increased in LPCAT1-depleted cells (1.24 ± 0.15 fold) while PL secretion was not modified. This indicates that LPCAT1-depleted cells have a slightly higher TAG secretion capacity compared to control. We concluded that LPCAT1 depletion in Huh-7.5.1 cells results in an altered lipid metabolism characterized by LD remodelling, increased intracellular TAG content, increased ApoB-containing lipoprotein secretion and increased TAG secretion capacity.

Next we examined the impact of LPCAT1 depletion on the hepatocellular lipid metabolism in the context of HCV infection. For all characteristics studied, similar effects were observed in LPCAT1-depleted Huh-7.5.1 cells irrespective of whether they were infected or not. Indeed, in infected Huh-7.5.1 cells LPCAT1 depletion led to a reduction in the mean number of LDs accompanied by a shift of the LD diameter distribution towards larger LDs (figure 6A-C), and increased both the intracellular amount of TAGs and the amount of secreted ApoB (figure 6D-E). Upon isopycnic iodixanol gradient ultracentrifugation of culture supernatant of these

cells, ApoB peaked at a higher buoyant density than the very low density (<1.006 g/ml) expected for VLDLs (figure 6F), consistent with the reported inability of the Huh-7 cell line to secrete genuine VLDLs.[25] Nevertheless, ApoB and ApoE, another important component of VLDLs, were both found in fractions with a density below 1.08 g/ml (figure 6F-G), i.e., in the density range of the excess of highly infectious HCV particles produced upon LPCAT1 depletion (figure 3D-E). Taken together, the results suggest that LPCAT1 depletion increases the secretion of TAG-rich lipoproteins and HCV particles associated with TAG-rich lipoproteins.

Validation of data in physiologically relevant PHH

Huh-7 sublines provide a most convenient and efficient HCV culture system, yet differ significantly from normal, quiescent, highly differentiated human adult hepatocytes and especially do not fully reproduce VLDL biogenesis.[25] In order to validate the data in a patho-physiologically relevant model, we used our HCV culture system in PHH, which produce genuine VLDLs and HCV particles whose properties mimic those of infectious HCV produced in vivo.[25] We first sought to determine whether HCV infection downregulates LPCAT1 expression in PHH as is the case in Huh-7.5.1 cells. Because PHH are primary cells, the infectivity titres reached upon JFH1-HCV inoculation were generally lower than those obtained in Huh-7.5.1 cells and varied from one donor of hepatocytes to another. When viral titres were below 5.10^4 ffu/ml, LPCAT1 mRNA amounts did not appear to be modified in PHH inoculated with HCV compared to naïve PHH (figure 7A). When higher titres were reached, however, a reduction of LPCAT1 mRNA amounts was observed, and a strong linear inverse relationship was found between LPCAT1 expression levels and HCV infectivity titres (figure 7B), consistent with the occurrence of HCV-induced transcriptional downregulation of LPCAT1 in PHH.

Next we investigated the impact of LPCAT1 depletion on HCV infectious cycle in PHH. For this, PHH were transfected with siRNA against LPCAT1 (siLPCAT1) versus GFP (siGFP), then inoculated with HCV. A significant decrease in LPCAT1 protein amount was observed in PHH transfected with siLPCAT1 compared to control (0.37 ± 0.05) (supplementary figure S2F), in the absence of cytotoxic effect (supplementary figure S3B). LPCAT1 depletion in PHH had no impact on HCV genome replication but increased the infectivity titre by almost 1 log (9.27 ± 5.60) (figure 7C), indicating an effect on virus morphogenesis. However, the viral load was not significantly modified, therefore the specific infectivity of viral particles produced was increased in LPCAT1-depleted PHH (7.87 ± 5.14). Upon isopycnic iodixanol gradient ultracentrifugation, the proportion of viral RNA-containing particles with a buoyant density below 1.08 g/ml was greater for HCV grown in PHH than for HCV grown in Huh-7.5.1 cells (compare siGFP in figure 7D with shLuc in figure 3B), as previously reported.[25] Nevertheless, a further shift of HCV RNA towards low buoyant density fractions was observed upon LPCAT1 depletion in PHH: the percentage of total viral load present below 1.09 g/ml was 47.01 ± 0.73% for LPCAT1-depleted cells as compared to 35.91 ± 0.68% for control cells (figure 7D). These low-density fractions contained the excess of highly infectious particles produced upon LPCAT1 depletion (figure 7E), also coinciding with an excess of ApoB (figure 7F). Thus, in PHH as in Huh-7.5.1 cells but even more strikingly, LPCAT1 depletion appeared to favour the morphogenesis of HCV particles of high specific infectivity correlating with low buoyant density.

DISCUSSION

The human hepatocyte is both the cell type specialized in the biogenesis of VLDLs, which permit export of TAGs into the circulation, and the primary replication site of HCV, which

circulates in the form of TAG-rich LVPs. Using two cell-culture-based models of human hepatocytes, we have here identified LPCAT1 as a host cell factor downregulated upon HCV infection. Depletion of this PL-remodelling enzyme was further found to affect TAG metabolism, leading to increased intracellular TAG content and eventually increased capacity of TAG secretion in the form of ApoB-containing lipoproteins. In infected hepatocytes this also resulted in increased production of HCV particles of lowest buoyant density, i.e., enriched in TAGs, which are those of highest infectivity. Thus, LPCAT1 downregulation by HCV appears as an original viral strategy to increase the virus specific infectivity. These data support the idea that HCV hijacks the hepatocellular lipid metabolism, which is devoted in particular to the efflux of TAGs in the form of VLDLs, for the benefit of LVP morphogenesis.

High-throughput profiling studies in the Huh-7/JFH1 model have suggested that HCV regulates the expression of host genes involved in a variety of hepatocellular processes, including liver lipid metabolism, at the transcriptional, translational and post-translational levels.[31-34] Our study reveals a decrease in the amounts of both LPCAT1 mRNA and protein in JFH1-infected Huh-7.5.1 cells, consistent with HCV-induced downregulation of LPCAT1 expression occurring at least partly at the transcriptional level. The PHH model is less suitable for such studies owing to lower levels of HCV infection and to the notorious autofluorescence of these cells that precludes in situ immunofluorescence analysis.[25] Our finding of a strong linear correlation between HCV infectivity titre and LPCAT1 mRNA amount is all the more striking in view of these limitations, supporting the occurrence of transcriptional downregulation of LPCAT1 by HCV in a patho-physiologically relevant model. Whereas LPCAT1 expression was unchanged in cells replicating an HCV subgenomic replicon, the sole expression of HCV core protein recapitulated the downregulation of LPCAT1 upon HCV infection. Although we cannot exclude an additional contribution of other HCV components, the virus core protein thus appears to play a major role in LPCAT1 downregulation. In fact

this is not surprising, as this multifunctional protein has been reported to regulate the expression of many host genes aside from its role as a structural component of the virion.[35 36] Furthermore, expression of HCV core protein alone is sufficient to alter the LD-associated proteome in various cell models.[37 38] Interestingly, HCV-induced changes in LD composition may involve different molecular mechanisms, including displacing of LD-associated proteins owing to the own localisation of HCV core protein to LDs, as reported for adipose differentiation-related protein,[39] and direct or indirect regulation of gene expression, as suggested here for LPCAT1.

In hepatic cells, an increased intracellular TAG content can result from increased fatty acid uptake, increased TAG synthesis, decreased fatty acid oxidation and/or decreased TAG-rich lipoprotein secretion. The latter mechanism cannot account for the increased intracellular TAG amount observed in LPCAT1-depleted cells because the secretion of newly synthesized TAGs was slightly increased in these cells. Another mechanism is suggested by the localisation of LPCAT1 to LDs. Like HCV core protein,[39] LPCAT1 may displace LD-associated proteins involved in lipid metabolism by its mere presence at the LD surface.[40] Furthermore, LPCAT1 is a PL-remodelling enzyme that catalyses the acylation of lysophosphatidylcholine into phosphatidylcholine,[21 41] the reverse reaction being performed by phospholipases A2 that may also be present at the LD surface.[20] Lysophosphatidylcholine and phosphatidylcholine have a different shape, and the alteration of the surface lipid composition may lead to changes in LD stability (e.g., LD fusion, LD interaction with membranes) and in protein binding.[19] Theoretically, LPCAT1 depletion should lead to an increased amount of lysophosphatidylcholine at the LD surface, a situation that does not favour LD fusion.[19] In fact, we observed fewer LDs of larger size, which may reflect LD fusion, in agreement with Moessinger et al.[22 23] Nevertheless, the modification of the PL monolayer composition induced by LPCAT1 depletion probably initiates a reaction cascade

that leads to impairment of protein interactions with the LD surface and further, possibly, with other organelles such as endoplasmic reticulum or mitochondria. Indeed, the trafficking of LD-associated proteins, including key enzymes of TAG metabolism, can be strongly modulated and the various mechanisms are only beginning to be understood as exemplified by recent reports.[16 42 43]

Besides the association of HCV particles with TAG-rich lipoproteins, another clinical feature that links HCV infection with the host lipid metabolism is the high prevalence of liver steatosis, which is partly attributable to a direct viral effect.[1 44] LPCAT1 depletion was shown here to cause both an increase in the net intracellular TAG content, i.e., steatosis, and an increase in the production of HCV particles associated with TAG-rich lipoproteins, thus illustrating a possible link between liver steatosis and LVP morphogenesis. However, HCV infection is not sufficient to induce steatosis in cell culture[45] and a variety of mechanisms have been suggested to account for HCV-induced steatosis, including inhibition of VLDL biogenesis which, unlike LPCAT1 downregulation, may explain the hypobetalipoproteinaemia frequently associated with liver steatosis in HCV-infected patients.[1-3 7 44 46] Thus, HCV-induced steatosis may only partially be accounted for by LPCAT1 downregulation. Furthermore, it remains uncertain whether steatosis per se has a role in LVP morphogenesis. The occurrence of liver steatosis in HCV-infected patients may simply represent the net result of the sum of perturbations of the host lipid metabolism that HCV induces primarily for the benefit of viral replication and LVP production added to non-viral steatogenic mechanisms of metabolic origin that can coexist to varying degrees in the same individual.

Upon LPCAT1 depletion in Huh-7.5.1 cells we observed an increased intracellular TAG content, an increased ApoB secretion and a slight but significant increase in the capacity of

secretion of newly synthesized TAGs, whereas a recent study reported no alteration of the total amount of lipids and a decreased secretion of both ApoB and lipids in LPCAT1-depleted Huh-7 cells.[23] This apparent discrepancy may be partly due to the different Huh-7 sublines but is more likely explained by the different experimental conditions used. Since ApoB is stabilized by lipids or otherwise degraded,[47] we cultured Huh-7.5.1 cells in medium supplemented with foetal calf serum, which contains lipids, and provided them with a physiological concentration of oleic acid (0.6 mM) to assess the TAG secretion capacity. By contrast, Moessinger et al.[23] cultured Huh-7 cells in serum-free medium for 3 days before lipid and ApoB analysis, and incubated them with only trace amounts of radiolabelled fatty acids for TAG secretion analysis. Under these conditions, the paucity of lipids available may have precluded TAG synthesis, hence ApoB stabilisation by lipidation and eventually lipoprotein formation.

LVPs found both in the liver and in the circulating blood of HCV-infected patients contain ApoB, the non-exchangeable Apo essential for VLDL scaffolding, and exchangeable Apos including ApoE.[4 5 48] The presence of ApoB and ApoE in the density range of the excess of HCV particles produced upon LPCAT1 depletion is compatible with their physical association but does not provide direct evidence for this hypothesis. Whereas a large body of evidence has underlined the essential role of ApoE both in production and infectivity of HCV, the literature contains conflicting reports as to whether ApoB is incorporated into HCV particles produced from Huh-7 cells and is necessary for production of infectious virus.[49-58] One possible source of discrepancies between published data may be the intrinsic inability of Huh-7 cell line to fully lipidate ApoB and hence secrete genuine VLDLs.[25] Our HCV culture system in PHH provides a more relevant model for readdressing these issues, yet the lower viral titres make it even more difficult to purify and characterize hybrid LVPs present within a large excess of non-viral lipoproteins.[6 8 25] Nevertheless, our identification of LPCAT1

depletion as a single mechanism that increases both VLDL and LVP secretion suggests that HCV usurps at least some of the mechanisms of VLDL biogenesis for LVP morphogenesis, even if ApoB per se is not incorporated into HCV particles.

HCV is a leading cause of chronic liver disease ranging from steatosis to cirrhosis and hepatocellular carcinoma. Treatment against HCV has entered a new era with the recent development of directly acting antivirals, yet these drugs have a prohibitive price, are intrinsically at risk for selection of resistant variants and may not cure a small proportion of hard-to-treat patients among whom those infected with genotype 3, the HCV genotype most clearly associated with virally induced steatosis.[44 59] By contrast, host-targeting agents with anti-HCV activity are expected to confer a high barrier to drug resistance and a pan-genotypic coverage, and therefore may appear as a useful complement to virus-targeting agents in most difficult-to-treat patients.[60] The intimate link of HCV with the host lipid metabolism designates lipid-modulating agents as putative antivirals.[3 61] Depending on their mechanism of action, however, a potential side effect of drugs in this therapeutic class may be to aggravate hepatic steatosis. With this in mind, targeting the LPCAT1-regulated lipid metabolism pathway in the opposite direction to that usurped by HCV may represent an attractive therapeutic approach because it is expected to reduce not only the viral titre but also hepatic steatosis.

ACKNOWLEDGEMENTS

We thank J. McLauchlan for the R308 antibody, R. Everett for silencing plasmids, F.V. Chisari for the Huh-7.5.1 cells and Cochin Imaging Facility for help with image analysis. Confocal microscopy was performed using the CICC facilities of UMR_S 1138.

FOOTNOTES

FB and ML or SD and ARR contributed equally to this work.

Contributors FB, ML, SD and ARR conceived and designed the study. FB, ML, VP and DR performed the experiments. FB, ML, VP, SD and ARR analysed and interpreted the data. FB, ML, SD and ARR drafted or wrote the manuscript. SD and ARR obtained funding. All authors approved the final version for submission.

Funding FB was the recipient of postdoctoral fellowships from ANRS (France REcherche Nord&sud Sida-hiv Hépatites) and EPHE. ML and VP were the recipients of doctoral or postdoctoral fellowships from ANRS, respectively. This work was supported by ANRS, Université Paris Descartes and Inserm.

Competing interests None.

REFERENCES

1. Negro F. Abnormalities of lipid metabolism in hepatitis C virus infection. *Gut* 2010;59:1279-87.
2. Syed GH, Amako Y, Siddiqui A. Hepatitis C virus hijacks host lipid metabolism. *Trends Endocrinol Metab* 2010;21:33-40.
3. Felmlee DJ, Hafirassou ML, Lefevre M, et al. Hepatitis C virus, cholesterol and lipoproteins--impact for the viral life cycle and pathogenesis of liver disease. *Viruses* 2013;5:1292-324.
4. Andre P, Komurian-Pradel F, Deforges S, et al. Characterization of low- and very-low-density hepatitis C virus RNA-containing particles. *J Virol* 2002;76:6919-28.
5. Nielsen SU, Bassendine MF, Burt AD, et al. Association between hepatitis C virus and very-low-density lipoprotein (VLDL)/LDL analyzed in iodixanol density gradients. *J Virol* 2006;80:2418-28.
6. Bartenschlager R, Penin F, Lohmann V, et al. Assembly of infectious hepatitis C virus particles. *Trends Microbiol* 2011;19:95-103.
7. Filipe A, McLauchlan J. Hepatitis C virus and lipid droplets: finding a niche. *Trends Mol Med* 2015;21:34-42.
8. Lindenbach BD. Virion assembly and release. *Curr Top Microbiol Immunol* 2013;369:199-218.
9. Walther TC, Farese RV, Jr. Lipid droplets and cellular lipid metabolism. *Annu Rev Biochem* 2012;81:687-714.
10. Gibbons GF, Islam K, Pease RJ. Mobilisation of triacylglycerol stores. *Biochim Biophys Acta* 2000;1483:37-57.
11. Olofsson SO, Bostrom P, Andersson L, et al. Lipid droplets as dynamic organelles connecting storage and efflux of lipids. *Biochim Biophys Acta* 2009;1791:448-58.
12. Fujimoto Y, Itabe H, Sakai J, et al. Identification of major proteins in the lipid droplet-enriched fraction isolated from the human hepatocyte cell line HuH7. *Biochim Biophys Acta* 2004;1644:47-59.
13. Mashek DG, Khan SA, Sathyanarayan A, et al. Hepatic lipid droplet biology: Getting to the root of fatty liver. *Hepatology* 2015;62:964-7.
14. Hodges BD, Wu CC. Proteomic insights into an expanded cellular role for cytoplasmic lipid droplets. *J Lipid Res* 2010;51:262-73.
15. Yang L, Ding Y, Chen Y, et al. The proteomics of lipid droplets: structure, dynamics, and functions of the organelle conserved from bacteria to humans. *J Lipid Res* 2012;53:1245-53.
16. Wilfling F, Thiam AR, Olarte MJ, et al. Arf1/COPI machinery acts directly on lipid droplets and enables their connection to the ER for protein targeting. *Elife* 2014;3:e01607.
17. Wilfling F, Wang H, Haas JT, et al. Triacylglycerol synthesis enzymes mediate lipid droplet growth by relocalizing from the ER to lipid droplets. *Dev Cell* 2013;24:384-99.
18. Sletten A, Seline A, Rudd A, et al. Surface features of the lipid droplet mediate perilipin 2 localization. *Biochem Biophys Res Commun* 2014;452:422-7.
19. Thiam AR, Farese RV, Jr., Walther TC. The biophysics and cell biology of lipid droplets. *Nat Rev Mol Cell Biol* 2013;14:775-86.
20. Penno A, Hackenbroich G, Thiele C. Phospholipids and lipid droplets. *Biochim Biophys Acta* 2013;1831:589-94.

21. Hishikawa D, Hashidate T, Shimizu T, et al. Diversity and function of membrane glycerophospholipids generated by the remodeling pathway in mammalian cells. *J Lipid Res* 2014;55:799-807.
22. Moessinger C, Kuerschner L, Spandl J, et al. Human lysophosphatidylcholine acyltransferases 1 and 2 are located in lipid droplets where they catalyze the formation of phosphatidylcholine. *J Biol Chem* 2011;286:21330-9.
23. Moessinger C, Klizaite K, Steinhagen A, et al. Two different pathways of phosphatidylcholine synthesis, the Kennedy Pathway and the Lands Cycle, differentially regulate cellular triacylglycerol storage. *BMC Cell Biol* 2014;15:43.
24. Li Z, Ding T, Pan X, et al. Lysophosphatidylcholine acyltransferase 3 knockdown-mediated liver lysophosphatidylcholine accumulation promotes very low density lipoprotein production by enhancing microsomal triglyceride transfer protein expression. *J Biol Chem* 2012;287:20122-31.
25. Podevin P, Carpentier A, Pene V, et al. Production of infectious hepatitis C virus in primary cultures of human adult hepatocytes. *Gastroenterology* 2010;139:1355-64.
26. Pene V, Hernandez C, Vauloup-Fellous C, et al. Sequential processing of hepatitis C virus core protein by host cell signal peptidase and signal peptide peptidase: a reassessment. *J Viral Hepat* 2009;16:705-15.
27. Carriere M, Pene V, Breiman A, et al. A novel, sensitive, and specific RT-PCR technique for quantitation of hepatitis C virus replication. *J Med Virol* 2007;79:155-60.
28. Chateau D, Pauquai T, Delers F, et al. Lipid micelles stimulate the secretion of triglyceride-enriched apolipoprotein B48-containing lipoproteins by Caco-2 cells. *J Cell Physiol* 2005;202:767-76.
29. Zhao Y, Chen YQ, Bonacci TM, et al. Identification and characterization of a major liver lysophosphatidylcholine acyltransferase. *J Biol Chem* 2008;283:8258-65.
30. Lindenbach BD, Meuleman P, Ploss A, et al. Cell culture-grown hepatitis C virus is infectious in vivo and can be recultured in vitro. *Proc Natl Acad Sci USA* 2006;103:3805-9.
31. Blackham S, Baillie A, Al-Hababi F, et al. Gene expression profiling indicates the roles of host oxidative stress, apoptosis, lipid metabolism, and intracellular transport genes in the replication of hepatitis C virus. *J Virol* 2010;84:5404-14.
32. Colman H, Le Berre-Scoul C, Hernandez C, et al. Genome-wide analysis of host mRNA translation during hepatitis C virus infection. *J Virol* 2013;87:6668-77.
33. Diamond DL, Syder AJ, Jacobs JM, et al. Temporal proteome and lipidome profiles reveal hepatitis C virus-associated reprogramming of hepatocellular metabolism and bioenergetics. *PLoS Pathog* 2010;6:e1000719.
34. Liu X, Wang T, Wakita T, et al. Systematic identification of microRNA and messenger RNA profiles in hepatitis C virus-infected human hepatoma cells. *Virology* 2010;398:57-67.
35. Khan M, Jahan S, Khaliq S, et al. Interaction of the hepatitis C virus (HCV) core with cellular genes in the development of HCV-induced steatosis. *Arch Virol* 2010;155:1735-53.
36. McLauchlan J. Properties of the hepatitis C virus core protein: a structural protein that modulates cellular processes. *J Viral Hepat* 2000;7:2-14.
37. Beilstein F, Bouchoux J, Rousset M, et al. Proteomic analysis of lipid droplets from Caco-2/TC7 enterocytes identifies novel modulators of lipid secretion. *PLoS One* 2013;8:e53017.
38. Sato S, Fukasawa M, Yamakawa Y, et al. Proteomic profiling of lipid droplet proteins in hepatoma cell lines expressing hepatitis C virus core protein. *J Biochem* 2006;139:921-30.

39. Boulant S, Douglas MW, Moody L, et al. Hepatitis C virus core protein induces lipid droplet redistribution in a microtubule- and dynein-dependent manner. *Traffic* 2008;9:1268-82.
40. Kory N, Thiam AR, Farese RV, Jr., et al. Protein Crowding Is a Determinant of Lipid Droplet Protein Composition. *Dev Cell* 2015;34:351-63.
41. Shindou H, Hishikawa D, Harayama T, et al. Generation of membrane diversity by lysophospholipid acyltransferases. *J Biochem* 2013;154:21-8.
42. Yeaman SJ. Hormone-sensitive lipase--new roles for an old enzyme. *Biochem J* 2004;379:11-22.
43. Suzuki M, Murakami T, Cheng J, et al. ELMOD2 is anchored to lipid droplets by palmitoylation and regulates adipocyte triglyceride lipase recruitment. *Mol Biol Cell* 2015;26:2333-42.
44. Goossens N, Negro F. Is genotype 3 of the hepatitis C virus the new villain? *Hepatology* 2014;59:2403-12.
45. Gottwein JM, Scheel TK, Hoegh AM, et al. Robust hepatitis C genotype 3a cell culture releasing adapted intergenotypic 3a/2a (S52/JFH1) viruses. *Gastroenterology* 2007;133:1614-26.
46. Serfaty L, Andreani T, Giral P, et al. Hepatitis C virus induced hypobetalipoproteinemia: a possible mechanism for steatosis in chronic hepatitis C. *J Hepatol* 2001;34:428-34.
47. Davidson NO, Shelness GS. Apolipoprotein B: mRNA editing, lipoprotein assembly, and presecretory degradation. *Annu Rev Nutr* 2000;20:169-93.
48. Nielsen SU, Bassendine MF, Martin C, et al. Characterization of hepatitis C RNA-containing particles from human liver by density and size. *J Gen Virol* 2008;89:2507-17.
49. Boyer A, Dumans A, Beaumont E, et al. The association of hepatitis C virus glycoproteins with apolipoproteins E and B early in assembly is conserved in lipoviral particles. *J Biol Chem* 2014;289:18904-13.
50. Chang KS, Jiang J, Cai Z, et al. Human apolipoprotein e is required for infectivity and production of hepatitis C virus in cell culture. *J Virol* 2007;81:13783-93.
51. Owen DM, Huang H, Ye J, et al. Apolipoprotein E on hepatitis C virion facilitates infection through interaction with low-density lipoprotein receptor. *Virology* 2009;394:99-108.
52. Hishiki T, Shimizu Y, Tobita R, et al. Infectivity of hepatitis C virus is influenced by association with apolipoprotein E isoforms. *J Virol* 2010;84:12048-57.
53. Lefevre M, Felmlee DJ, Parnot M, et al. Syndecan 4 is involved in mediating HCV entry through interaction with lipoviral particle-associated apolipoprotein E. *PLoS One* 2014;9:e95550.
54. Catanese MT, Uryu K, Kopp M, et al. Ultrastructural analysis of hepatitis C virus particles. *Proc Natl Acad Sci USA* 2013;110:9505-10.
55. Gastaminza P, Cheng G, Wieland S, et al. Cellular determinants of hepatitis C virus assembly, maturation, degradation, and secretion. *J Virol* 2008;82:2120-9.
56. Huang H, Sun F, Owen DM, et al. Hepatitis C virus production by human hepatocytes dependent on assembly and secretion of very low-density lipoproteins. *Proc Natl Acad Sci USA* 2007;104:5848-53.
57. Jiang J, Luo G. Apolipoprotein E but not B is required for the formation of infectious hepatitis C virus particles. *J Virol* 2009;83:12680-91.
58. Merz A, Long G, Hiet MS, et al. Biochemical and morphological properties of hepatitis C virus particles and determination of their lipidome. *J Biol Chem* 2011;286:3018-32.
59. Pawlotsky JM, Feld JJ, Zeuzem S, et al. From non-A, non-B hepatitis to hepatitis C virus cure. *J Hepatol* 2015;62:S87-99.

60. Baugh JM, Garcia-Rivera JA, Gallay PA. Host-targeting agents in the treatment of hepatitis C: a beginning and an end? *Antiviral Res* 2013;100:555-61.
61. Bassendine MF, Sheridan DA, Felmlee DJ, et al. HCV and the hepatic lipid pathway as a potential treatment target. *J Hepatol* 2011;55:1428-40.

FIGURE LEGENDS

Figure 1 HCV infection downregulates LPCAT1 in Huh-7.5.1 cells. Cells were inoculated or not with HCV, and analysed 3 days later. (A) Cells were lysed for western blot analysis. (Left) A representative western blot is shown. (Right) LPCAT1 protein amounts were normalised to those of actin. The means ± SEM of three independent experiments performed in triplicate are shown. (B) Cells inoculated with HCV were stained for LPCAT1 (LPCAT1), HCV core protein (Core) and LDs (BODIPY), and examined by confocal microscopy. (Left) A merged image is shown (Merge); white and empty arrowheads indicate infected and non-infected cells, respectively. (Right) LPCAT1 signals were quantified for at least 80 cells per condition within three independent experiments.

Figure 2 Mechanism of HCV-induced downregulation of LPCAT1. Huh-7.5.1 cells were (A and B) electroporated or not with HCV subgenomic replicon (SGR), or (C and D) transfected with HCV core-encoding plasmid (pFlag-Core2a) or empty plasmid (pFlag-) as control, and analysed 2 days later. (A and C) Cells were lysed for RT-qPCR analysis. Expression of LPCAT1 transcript was normalised to that of human ribosomal protein L19 transcript. The means ± SEM of three independent experiments performed in triplicate are shown. (B) Cells electroporated with HCV subgenomic replicon were stained for LPCAT1 (LPCAT1), HCV NS3 protein (NS3) and LDs (BODIPY), and examined by confocal microscopy. (Left) A merged image is shown (Merge); white and empty arrowheads indicate NS3-positive and -negative cells, respectively. (Right) LPCAT1 signals were quantified for at least 80 cells per condition within three independent experiments. (D) Cells transfected with HCV core-encoding plasmid were stained for LPCAT1 (LPCAT1), HCV core protein (Core) and LDs (BODIPY), and examined by confocal microscopy. (Left) A merged image is shown (Merge); white and empty arrowheads indicate core-positive and -negative cells, respectively.

(Right) LPCAT1 signals were quantified for at least 80 cells per condition within three independent experiments. Of note, the proportion of core-positive cells among the total population of cells transfected with HCV core-encoding plasmid was approximately 15%.

Figure 3 LPCAT1 depletion in Huh-7.5.1 cells increases production of HCV particles with high specific infectivity and low density. Cells were transduced with lentiviral vectors encoding shLuc or shLPCAT1, and inoculated with HCV 3 days later. (A) Cells were lysed at day 1 post-inoculation for quantification of negative-strand HCV RNA, and culture supernatants were collected at day 3 post-inoculation for determination of infectivity titre and viral load, then calculation of specific infectivity. The means ± SEM of three to eight independent experiments performed in triplicate are shown. (B-E) Culture supernatants were subjected to isopycnic iodixanol gradient ultracentrifugation, and fractions were probed for (B) viral load, (C) specific infectivity, (D) ApoB and (E) ApoE. All graphs (B-E) are from the same representative experiment shown, and are aligned with one another (a dotted line has been placed at the density of 1.08 g/ml).

Figure 4 LPCAT1 depletion in Huh-7.5.1 cells alters lipid metabolism. Cells were transduced with lentiviral vectors encoding shLuc or shLPCAT1. Three days later, (A) cells were stained for LDs; LDs were (B) counted and (C) analysed for size distribution; (D) intracellular TAG amount and (E) secreted ApoB were quantified. The number and size of LDs were analysed for at least 10 cells per condition within three independent experiments. The means ± SEM of three independent experiments performed in triplicate are shown.

Figure 5 LPCAT1 depletion in Huh-7.5.1 cells increases TAG secretion capacity. Cells were transduced with lentiviral vectors encoding shLuc or shLPCAT1, and cultured for the last 24 h with oleic acid/BSA containing [1-^{14}C] oleic acid as a tracer. Lipids from cells and media were extracted and fractionated by thin layer chromatography, and radioactivity in

TAGs and PLs was quantified. The means ± SEM of three independent experiments performed in triplicate are shown.

Figure 6 LPCAT1 depletion in HCV-infected Huh-7.5.1 cells alters lipid metabolism. Cells were transduced with lentiviral vectors encoding shLuc or shLPCAT1, inoculated with HCV 3 days later and cultured for 3 more days. (A) Cells were stained for HCV core protein (Core) and LDs (BODIPY), and merged images are shown (Merge). LDs were (B) counted and (C) analysed for size distribution. (D) Intracellular TAG amount and (E) secreted ApoB were quantified. (F and G) Culture supernatants were subjected to isopycnic iodixanol gradient ultracentrifugation, and fractions were analysed for (F) ApoB and (G) ApoE by (bottom) western blot and (top) ELISA. The number and size of LDs were analysed for at least 10 cells per condition within three independent experiments. The means ± SEM of three independent experiments performed in triplicate are shown.

Figure 7 HCV infection downregulates LPCAT1 in PHH and LPCAT1 depletion in these cells increases production of HCV particles with high specific infectivity and low density. (A and B) PHH were inoculated or not with HCV, and analysed 6 days later for LPCAT1 mRNA amounts and infectivity titres; (B) linear regression between these two variables. (C-F) PHH were transfected with siGFP or siLPCAT1, and inoculated with HCV 3 days later: (C) same legend as figure 3A, (D, E and F) same legend as figure 3B, 3C and 3D, respectively. The means ± SEM of three to five independent experiments (i.e., with PHH from different donors) performed in triplicate are shown.

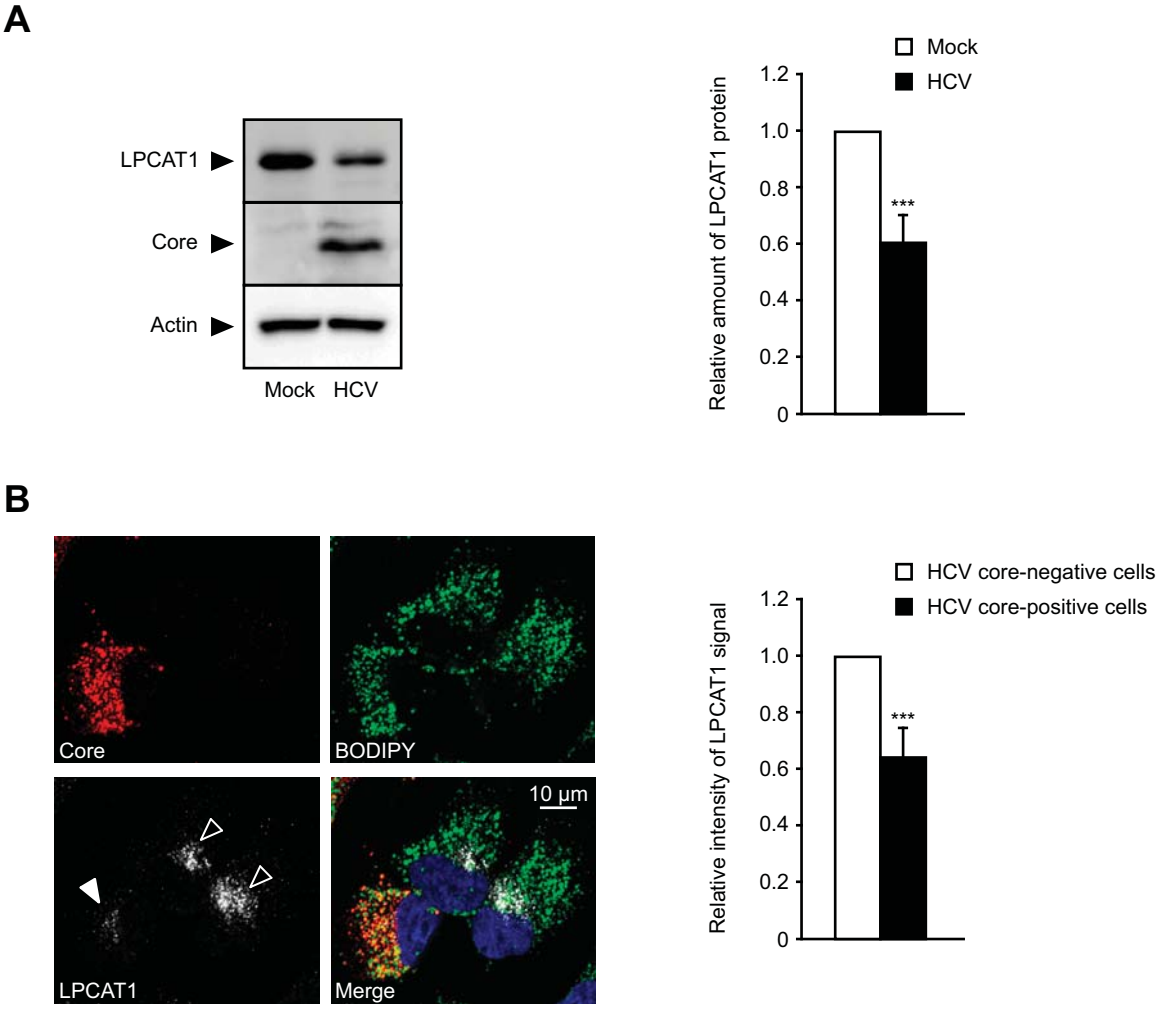
A
LPCAT1
Core
Actin
Mock
HCV
Mock
HCV
Relative amount of LPCAT1 protein
1.2
1.0
0.8
0.6
0.4
0.2
0
***
B
Core
BODIPY
10 μm
LPCAT1
Merge
HCV core-negative cells
HCV core-positive cells
Relative intensity of LPCAT1 signal
1.2
1.0
0.8
0.6
0.4
0.2
0
***

Figure 1

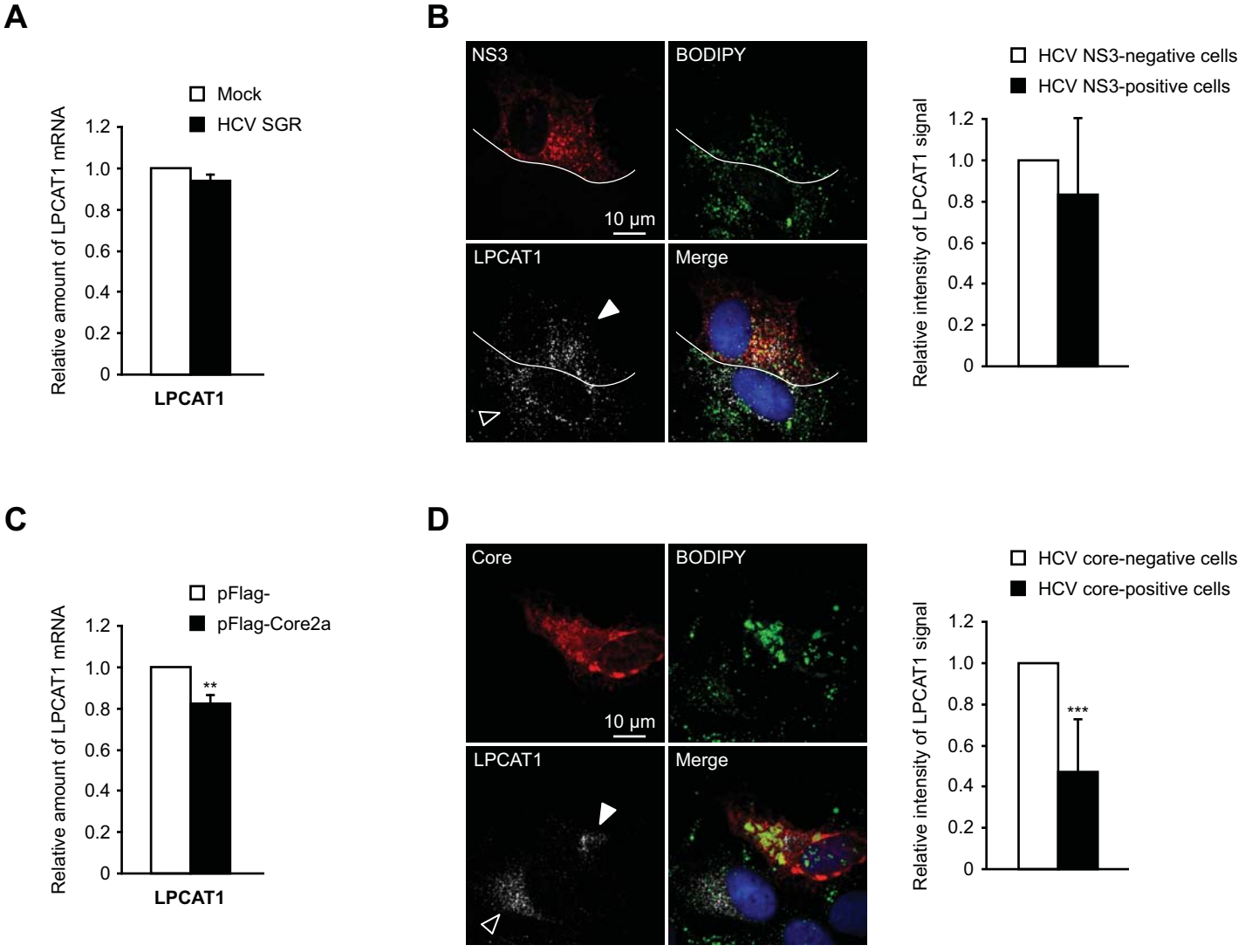
A
Mock
HCV SGR
Relative amount of LPCAT1 mRNA
1.2
1.0
0.8
0.6
0.4
0.2
0
LPCAT1
B
NS3
BODIPY
10 μm
LPCAT1
Merge
HCV NS3-negative cells
HCV NS3-positive cells
Relative intensity of LPCAT1 signal
C
pFlag-
pFlag-Core2a
**
Relative amount of LPCAT1 mRNA
LPCAT1
D
Core
BODIPY
10 μm
LPCAT1
Merge
HCV core-negative cells
HCV core-positive cells
***
Relative intensity of LPCAT1 signal

Figure 2

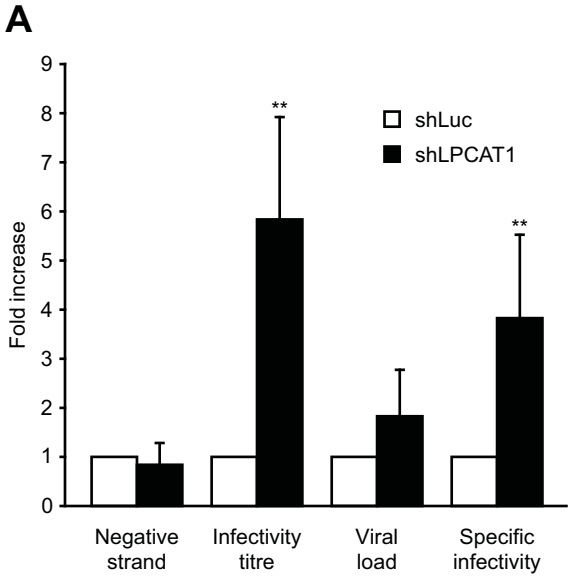
A
Fold increase
shLuc
shLPCAT1
**
**
Negative strand
Infectivity titre
Viral load
Specific infectivity

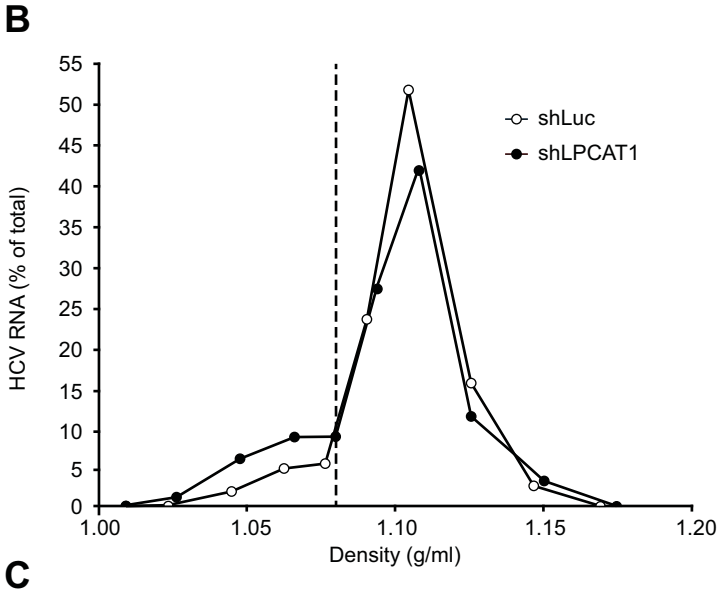
B
HCV RNA (% of total)
shLuc
shLPCAT1
Density (g/ml)

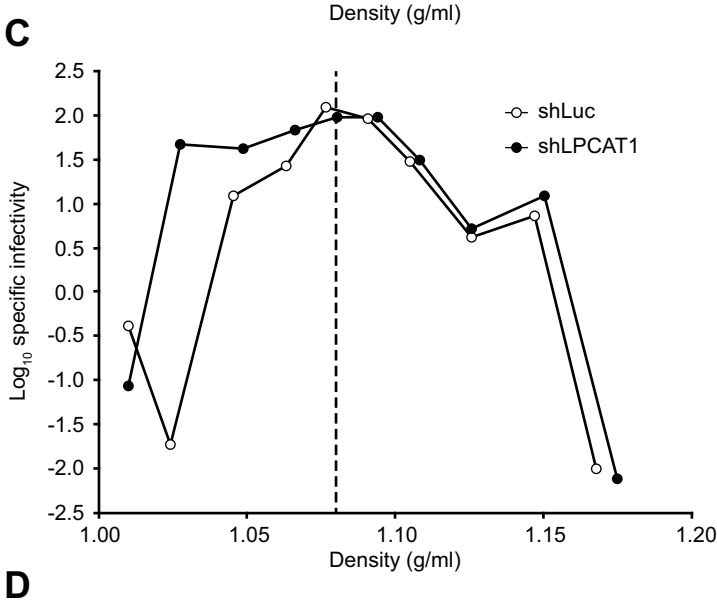
C
Log10 specific infectivity
shLuc
shLPCAT1
Density (g/ml)

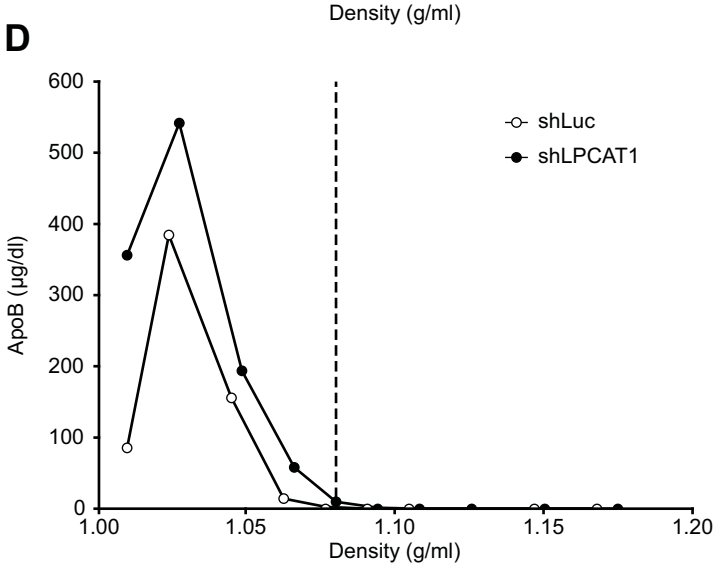
D
ApoB (µg/dl)
shLuc
shLPCAT1
Density (g/ml)

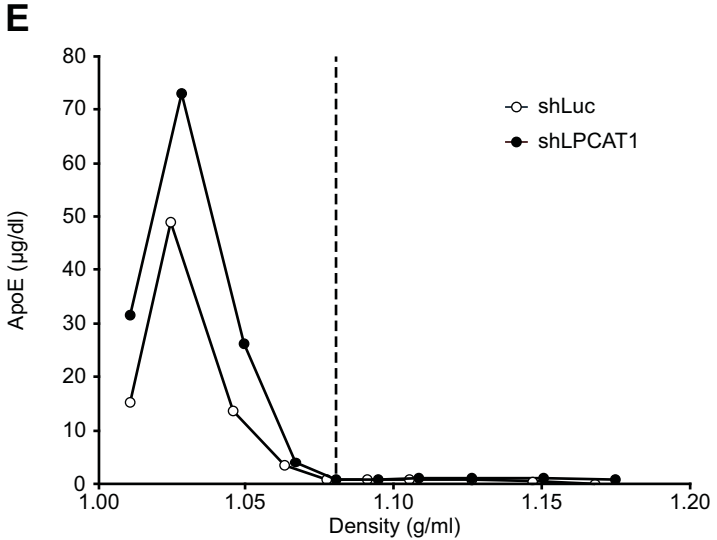
E
ApoE (µg/dl)
shLuc
shLPCAT1
Density (g/ml)

Figure 3

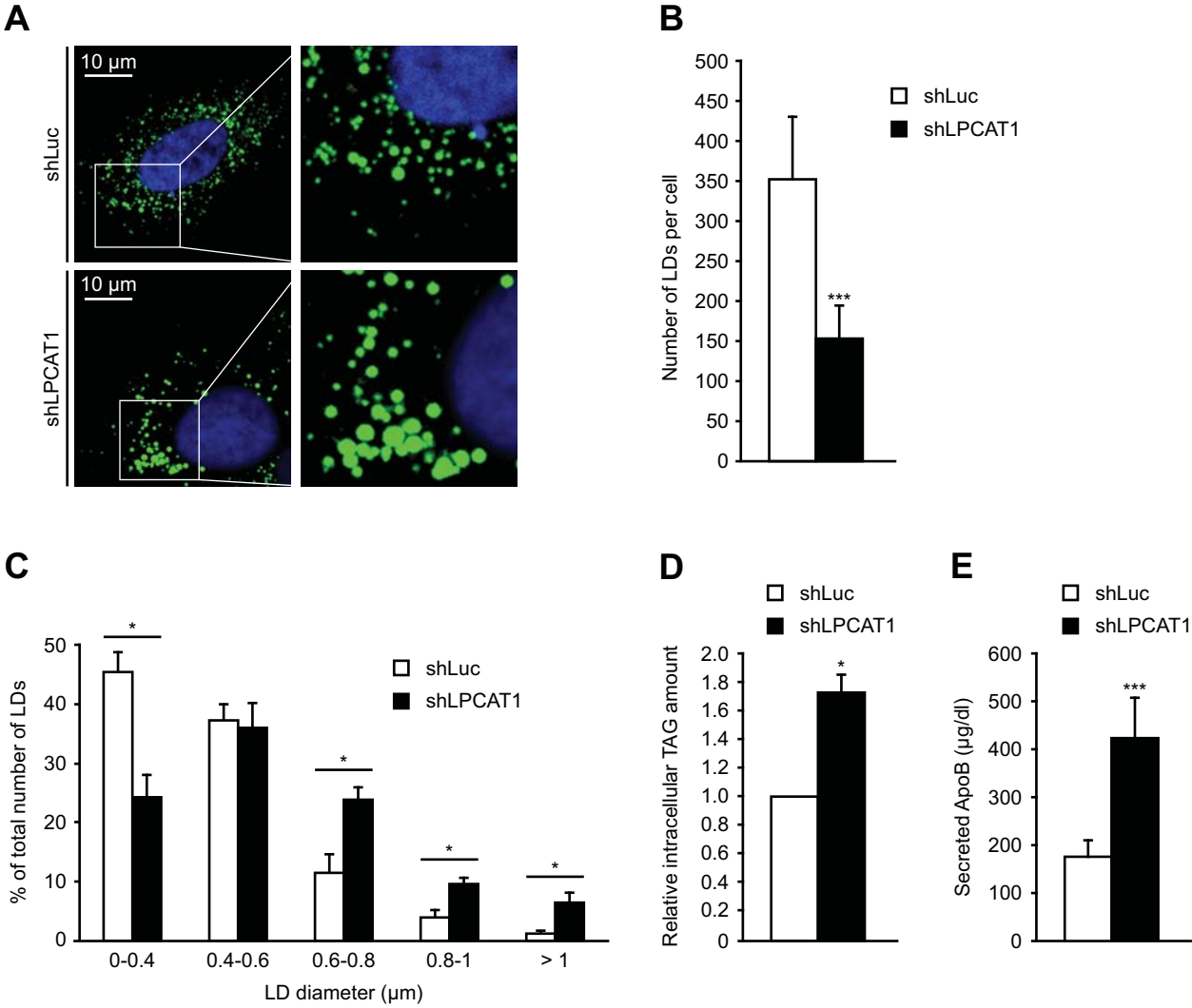
A
10 µm
shLuc
10 µm
shLPCAT1
B
Number of LDs per cell
shLuc
shLPCAT1
***
C
% of total number of LDs
shLuc
shLPCAT1
0-0.4
0.4-0.6
0.6-0.8
0.8-1
> 1
LD diameter (µm)
D
Relative intracellular TAG amount
shLuc
shLPCAT1
E
Secreted ApoB (µg/dl)
shLuc
shLPCAT1

Figure 4

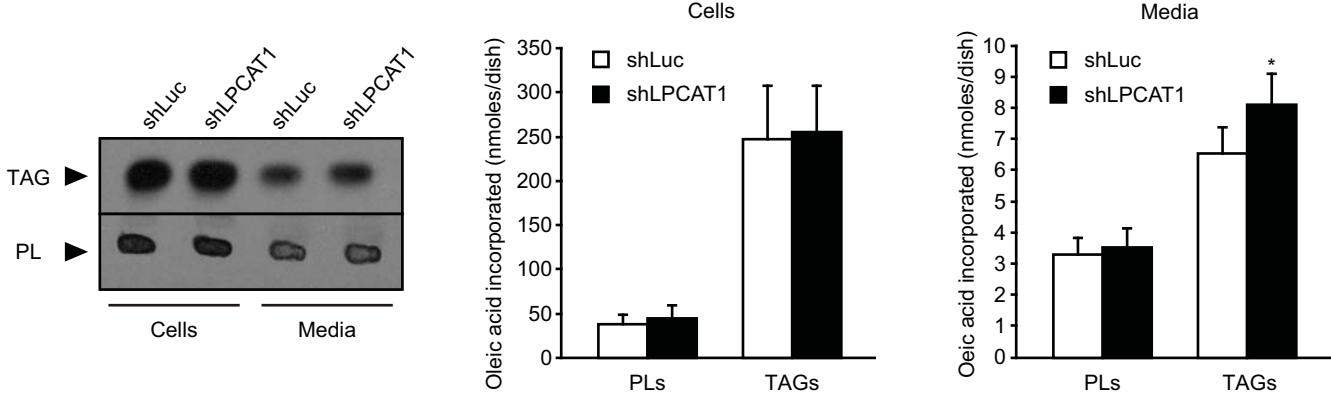
shLuc
shLPCAT1
shLuc
shLPCAT1
TAG
PL
Cells
Media
Cells
Oleic acid incorporated (nmoles/dish)
shLuc
shLPCAT1
PLs
TAGs
Media
Oeic acid incorporated (nmoles/dish)
shLuc
shLPCAT1
*
PLs
TAGs

Figure 5

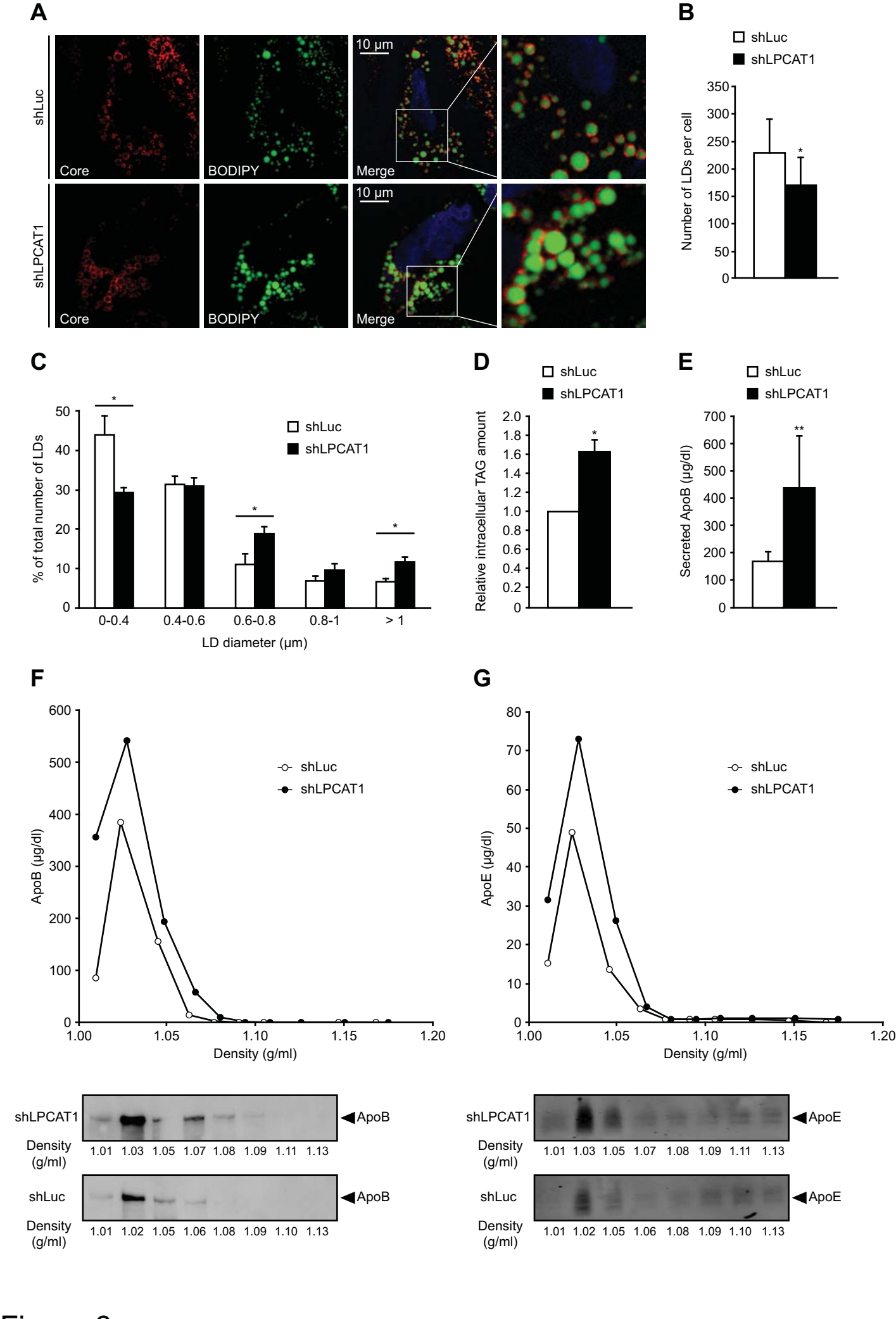
A
shLuc
shLPCAT1
Core
BODIPY
Merge
10 μm
B
shLuc
shLPCAT1
Number of LDs per cell
C
% of total number of LDs
LD diameter (μm)
0-0.4
0.4-0.6
0.6-0.8
0.8-1
> 1
D
Relative intracellular TAG amount
E
Secreted ApoB (μg/dl)
F
ApoB (μg/dl)
Density (g/ml)
G
ApoE (μg/dl)
Density (g/ml)
ApoB
ApoE
Density (g/ml)

Figure 6

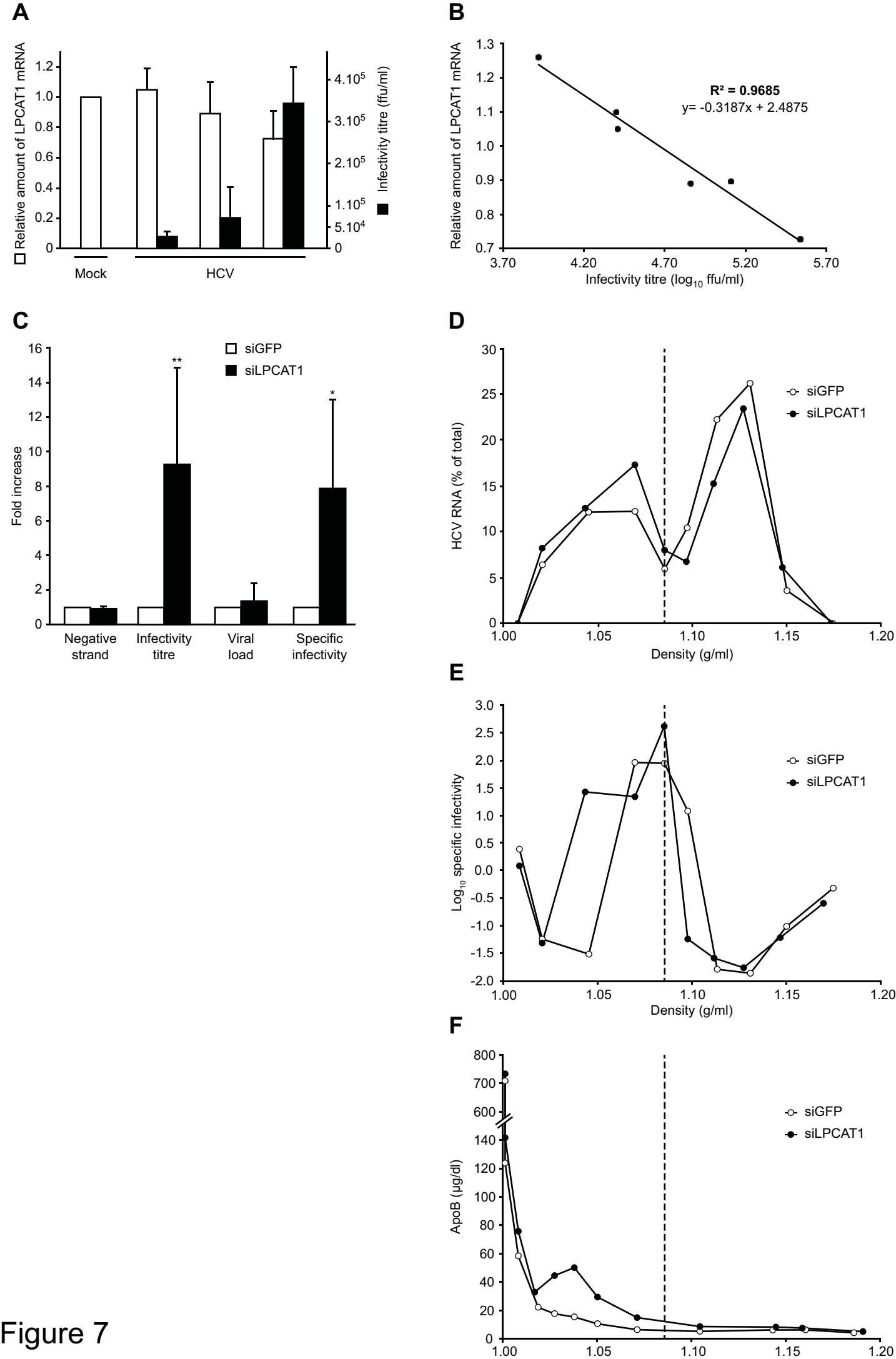
A
Relative amount of LPCAT1 mRNA
Infectivity titre (ffu/ml)
Mock
HCV
B
Relative amount of LPCAT1 mRNA
R² = 0.9685
y= -0.3187x + 2.4875
Infectivity titre (log10 ffu/ml)
C
siGFP
siLPCAT1
Fold increase
Negative strand
Infectivity titre
Viral load
Specific infectivity
D
siGFP
siLPCAT1
HCV RNA (% of total)
Density (g/ml)
E
siGFP
siLPCAT1
Log10 specific infectivity
Density (g/ml)
F
siGFP
siLPCAT1
ApoB (µg/dl)

Figure 7

SUPPLEMENTARY MATERIAL TO:

Lysophosphatidylcholine acyltransferase 1 is downregulated by hepatitis C virus: impact on production of lipo-viro-particles

Frauke Beilstein[1,2,†], Matthieu Lemasson[3,†], Véronique Pène[3], Dominique Rainteau[4], Sylvie Demignot[1,2,‡], Arielle R. Rosenberg[3,5,‡]

[†] or [‡] These authors contributed equally to this work.

[1]Sorbonne Universités, UPMC Univ. Paris 06, Inserm, Université Paris Descartes, Sorbonne Paris Cité, UMR_S 1138, Centre de recherche des Cordeliers, F-75006, Paris, France; [2]EPHE, Ecole Pratique des Hautes Etudes, PSL Research University, Laboratoire de Pharmacologie Cellulaire et Moléculaire, F-75006, Paris, France; [3]Université Paris Descartes, EA 4474 « Hepatitis C Virology», F-75014, Paris, France; [4]UPMC Univ. Paris 06, ERL INSERM U 1157/UMR 7203, F-75012, Paris, France; [5]AP-HP, Groupe Hospitalier Cochin, Service de Virologie, F-75014, Paris, France

SUPPLEMENTARY MATERIALS AND METHODS

Antibodies

The antibodies against LPCAT1 (HPA022268) and actin (A3853) were obtained from Sigma-Aldrich (St. Louis, MO, USA), the anti-ApoE antibody (AB947) was from Millipore (Darmstadt, Germany), and the monoclonal antibodies against HCV core protein (C7-50) and NS3 protein (AB65407) used for confocal microscopy were from Abcam (Cambridge, UK). The anti-HCV core protein antibody (R308) used for western blots was generously provided by J. McLauchlan[1] and the monoclonal antibody against human ApoB (1D1) was from the Heart Institute of the University of Ottawa (Canada). Secondary antibodies were appropriate Alexa Fluor 568- and 633-conjugated antibodies and horseradish peroxidase (HRP)-conjugated IgGs (GE Healthcare, Chalfont St. Giles, UK).

Cell culture

HEK 293T cells were grown at 37°C in Dulbecco's modified Eagle medium (DMEM, Life technologies, Carlsbad, CA, USA) supplemented with 10% heat-inactivated foetal calf serum (FCS, GE Healthcare).

Huh-7.5.1 cells[2] (a kind gift from F.V. Chisari, the Scripps Research Institute, La Jolla, CA, USA) were grown in DMEM supplemented with 10 mM hydroxyethyl piperazineethanesulfonic acid (HEPES) buffer (pH 7.3), 1% non-essential amino acids, 2 mM L-glutamine, 100 µg/ml streptomycin, 100 U/ml penicillin (all Life technologies) and 10% heat-inactivated FCS, at 37°C in a humidified 5% CO_2 atmosphere.

PHH freshly isolated from HCV-seronegative adult patients were purchased from Biopredic (Rennes, France) and maintained in primary culture as described previously.[3] Briefly, PHH were resuspended in complete medium consisting of Leibovitz's L-15 medium (Invitrogen,

Cergy Pontoise, France) supplemented with 26 mM $NaHCO_3$, 100 μg/ml streptomycin, 100 U/ml penicillin, 100 IU/l insulin (Novo Nordisk, Bagsvaerd, Denmark) and 10% heat-inactivated FCS, and seeded onto 6-well plates pre-coated with calf skin type I collagen (Sigma-Aldrich) at a density of 1.6 x 10^5 viable cells/cm^2. The medium was replaced 16 h later with fresh complete medium supplemented with 1 μM hydrocortisone hemisuccinate (SERB, Paris, France), and cells were left in this medium until HCV inoculation or siRNA transfection. The cultures were maintained in complete medium at 37°C in a humidified 5% CO_2 atmosphere.

HCV infection

A high-titre stock of JFH1-HCV[4] was produced as described previously.[3] Huh-7.5.1 cells and PHH were inoculated at a multiplicity of infection of 0.2 and 2 ffu per cell, respectively. The culture medium was replaced with the inoculum diluted in the smallest volume of fresh medium sufficient for covering the cells. The inoculum was removed after a 4-h incubation at 37°C. Cells were washed three times with phosphate-buffered saline (PBS) and maintained in culture for the indicated times post-inoculation.

Subgenomic replicon transfection

The HCV subgenomic R-Luc/JFH-1-replicon (SGR) was provided by Taka Kato (NIID, Tokyo, Japan).[5] The plasmid was linearized at the XbaI site, purified by phenol-chloroform-isoamyl alcohol extraction and used as template for in vitro transcription by T7 RNA polymerase with the RiboMAX™ large scale RNA production system (Promega), according to the manufacturer's instructions. The resulting RNA were purified by use of TRIzol RNA isolation reagent (Life Technologies), and their quality and quantity were evaluated by electrophoresis and NanoDrop spectrophotometry (Thermo Scientific). Huh-7.5.1 cells in mid-log phase were detached with trypsin, and resuspended at 10^7 cells/ml in Opti-MEM^R

(Invitrogen). Then 400 µl of this suspension were mixed with 10 µg of in vitro transcribed RNA in an electroporation cuvette (0.4-cm gap), and pulsed once at 0.28 kV, 975 µF, in a Gene PulserR II electroporator (Bio-Rad, Marne La Coquette, France). Immediately after electroporation, cells were plated at a density of 5.10^4 cells/cm^2 and maintained in culture for the indicated times post-electroporation.

Plasmid cloning and transfection

The pUC/JFH-1 plasmid was provided by Takaji Wakita (NIID, Tokyo, Japan).[4] HCV core sequence was amplified from pUC/JFH-1 plasmid using the following primers: CGAAGCTTATGAGCACAAATCCTAAACCTCAAAGAAAAACC and CGGAATTCTTA AGCAGAGACCGGAACGGTG. The plasmid pFLAG-Core2a was generated by cloning the HCV core amplicon into p3xFLAG-Myc-CMV-26 expression vector (Sigma-Aldrich) between *Hind*III and *Eco*RI restriction sites.

The plasmids pcDNA3.1, pcDNA3.1-LPCAT1-WT and pcDNA3.1-LPCAT1-RESCUE were provided by Life Technologies.

All plasmid transfections were performed using Lipofectamine 2000 transfection reagent (Life Technologies), according to the manufacturer's instructions.

Gene silencing

The use of lentiviral vectors expressing small hairpin RNA (shRNA) was described previously.[6] Briefly, HEK 293T cells were co-transfected with three plasmids: pVSV-G, pCMVDR8.91 (provided by D. Trono [http://ww1.tronolab.com/]) and the shRNA-encoding plasmid based on pLKO.1puro (the 19-nucleotide sequences used for silencing LPCAT1 and luciferase were GGAAGATCACATTCGCTGA and GTGCGTTGCTAGTACCAAC, respectively). The culture supernatant containing recombinant lentivirus was harvested 3 days

post-transfection and used to transduce Huh-7.5.1 cells in the presence of hexadimethrine bromide (5 µg/ml polybrene, Sigma-Aldrich). After overnight incubation, the cells were placed in selective medium containing 2 µg/ml puromycin (Sigma-Aldrich) for 1 day, then culture supernatant was changed for fresh selective medium and cells were cultured in this medium 1 additional day. Finally, culture supernatant was replaced by complete medium and the next day cells were inoculated or not with HCV.

Three days post-seeding, PHH were transfected with 20 nM siRNA (Eurogentec) using RiboCellin (BioCellChallenge) according to the manufacturer's instructions. The siRNA sequences were GGACCUGCCUAAUUACCUUtt and GAACGGCAUCAAGGUGAACtt for LPCAT1 and GFP, respectively. After 3 days, cells were washed with PBS then inoculated with HCV.

RT-qPCR

Total RNA was isolated from cells using TRI Reagent (Molecular Research Center, Cincinnati, OH, USA), according to the manufacturer's protocol. Reverse transcription was performed with 1 µg of total RNA in a total volume of 20 µl. PCR reactions were performed in quadruplicate using a Light-cycler instrument (Roche, Basel, Switzerland). For each reaction, a 1:400 final dilution of the reverse transcription product was used with 0.4 µM (final concentration) of each primer in SYBR Green I master mixture (Roche). PCR conditions were one step of denaturation (8 min at 95 °C) followed by 45 cycles (each cycle consisting of 10 s at 95 °C, 10 s at 60 °C and 10 s at 72 °C). Expression of LPCAT1, LPCAT3 or LPCAT4 transcripts was normalised to that of human ribosomal protein L19 transcript. The following oligonucleotide primers were used (for each couple, the forward primer is listed first and the reverse primer second): L19 (AAGATCGATCGCCACATGTAT / TGCGTGCTTCCTTGGTCTTAG), LPCAT1 (CGATGTCCTCCATCGTGA /

GGCCGTATATACTGGATCAGAGTT), LPCAT3 (ACCAGGAAAGATACCAAACAGC / GGTAGAAAAGGCCCAGACTCA) and LPCAT4 (CCCTTCGTGCATGAGTTACA / ATAAAGGCCAGAAGCACTCG).

Western blotting

Proteins were resolved on 10% (5% for ApoB) sodium dodecyl sulphate-polyacrylamide gels and transferred to nitrocellulose membrane (Hybond ECL, GE Healthcare). Blots were blocked for 30 min with 5% skimmed milk in TBS-Tween consisting of 20 mM Tris-HCl (pH 7.6), 137 mM NaCl and 0.1% Tween 20, then probed with primary antibodies diluted in TBS-Tween containing 1% skimmed milk followed by appropriate peroxidase-conjugated secondary antibodies. Actin was used as a loading control. Blots were developed by enhanced chemiluminescence using ECL reagent (GE Healthcare). Bands were visualised using the Image Reader LAS-4000 (Fujifilm, Tokyo, Japan) and quantified using ImageJ software.

Confocal microscopy

Cells on glass coverslips were fixed with 4% paraformaldehyde for 10 min at room temperature and, after two washes with PBS, permeabilized with 0.03% saponin in PBS for 30 min. After incubation with antibodies against LPCAT1 and HCV core protein (C7-50) or HCV NS3 protein for 1 h at room temperature, the coverslips were washed three times with PBS and incubated with appropriate secondary antibodies (Alexa Fluor 568–conjugated anti-rabbit IgG and Alexa Fluor 633–conjugated anti-mouse IgG, respectively) for 1 additional hour. After three washes with PBS, cells were stained for neutral lipids by a 10-min incubation with 10 μg/ml BODIPY 493/503 (Life Technologies) to visualise LDs and mounted in Fluoprep (BioMérieux, Marcy l'Etoile, France) containing 1 μg/ml 4′,6-diamidino-2-phenylindole dihydrochloride (DAPI, Sigma-Aldrich). The samples were examined using a Zeiss LSM 710 Meta confocal microscope. ImageJ software was used for

quantification of signal intensity and for measurement of LD number and size, using data from three independent experiments and at least 10 different pictures per condition.

ApoB and ApoE quantification

ApoB and ApoE levels in filtered culture supernatants or iodixanol gradient fractions were quantified by using the total human ApoB or ApoE ELISA assay from ALerCHEK (Springvale, MA, USA), respectively, according to the manufacturer's instructions.

Virological analyses

Intracellular amounts of negative-strand HCV RNA were quantified by a RT-qPCR technique described previously.[7] HCV RNA amounts in filtered cell culture supernatants or in iodixanol gradient fractions were quantified by the Abbott RealTime HCV viral load assay and expressed as international units (IU)/ml; infectivity titres were assessed by focus-formation assay and expressed as ffu/ml.[3 8] Specific infectivity values were calculated as follows: 10^3 x infectivity titre (ffu)/HCV RNA level (IU). The buoyant densities of viral particles were determined by isopycnic iodixanol gradient ultracentrifugation, as previously described.[3]

Lipid analyses

Quantification of the TAG mass was done on dried lipids extracted from cells with chloroform/methanol (2:1, v/v) using the PAP150TG kit (BioMérieux) according to the manufacturer's instructions with the following modifications: 0.5 ml of the buffer provided with the kit was added to the dried lipids and tubes were sonicated for 10 s in a water bath sonicator; then 0.5 ml of the 2-fold concentrated kit reagent was added and absorbance was measured after a 1-h incubation at 37°C.

The analysis of lipid secretion capacity was performed as described previously.[9] Briefly [1-^{14}C] oleic acid (Perkin Elmer Life Sciences, Waltham, MA, USA) (1 μCi per ml of final medium to prepare) was added to non-radioactive oleic acid (6 μl from a 100 mM stock solution in chloroform/methanol 2:1 (v/v) per ml of final medium to prepare) before drying under a stream of nitrogen, followed by incubation with FCS (0.1 ml per ml of final medium to prepare) for 1 h at 37 °C to obtain oleic acid in complex with BSA. The mixture was adjusted to 1 ml with culture medium without serum and supplied to the cells for the last 24 h of culture. Lipids were extracted from cells and media and fractionated by thin layer chromatography (TLC). The radioactive bands of the TLC plates were excised and the radioactivity was quantified by liquid-scintillation counting to evaluate the incorporation of [1-^{14}C] oleic acid into lipids. For normalisation, protein concentration of cell lysates was measured using the BC Assay (Interchim, Montluçon, France), according to the manufacturer's instructions.

Cytotoxicity assay

To assess the potential cytotoxicity of LPCAT1 silencing, the activity of lactate dehydrogenase released into culture supernatants was measured in triplicate using the CytoTox 96 Non-Radioactive Cytotoxicity Assay (Promega, Madison, WI, USA), according the recommendations of the manufacturer.

References

1. Targett-Adams P, Chambers D, Gledhill S, et al. Live cell analysis and targeting of the lipid droplet-binding adipocyte differentiation-related protein. *J Biol Chem* 2003;278:15998-6007.
2. Zhong J, Gastaminza P, Cheng G, et al. Robust hepatitis C virus infection in vitro. *Proc Natl Acad Sci U S A* 2005;102:9294-9.
3. Podevin P, Carpentier A, Pene V, et al. Production of infectious hepatitis C virus in primary cultures of human adult hepatocytes. *Gastroenterology* 2010;139:1355-64.
4. Wakita T, Pietschmann T, Kato T, et al. Production of infectious hepatitis C virus in tissue culture from a cloned viral genome. *Nat Med* 2005;11:791-6.
5. Kato T, Date T, Miyamoto M, et al. Efficient replication of the genotype 2a hepatitis C virus subgenomic replicon. *Gastroenterology* 2003;125:1808-17.
6. Everett RD, Rechter S, Papior P, et al. PML contributes to a cellular mechanism of repression of herpes simplex virus type 1 infection that is inactivated by ICP0. *J Virol* 2006;80:7995-8005.
7. Carriere M, Pene V, Breiman A, et al. A novel, sensitive, and specific RT-PCR technique for quantitation of hepatitis C virus replication. *J Med Virol* 2007;79:155-60.
8. Pene V, Hernandez C, Vauloup-Fellous C, et al. Sequential processing of hepatitis C virus core protein by host cell signal peptidase and signal peptide peptidase: a reassessment. *J Viral Hepat* 2009;16:705-15.
9. Chateau D, Pauquai T, Delers F, et al. Lipid micelles stimulate the secretion of triglyceride-enriched apolipoprotein B48-containing lipoproteins by Caco-2 cells. *J Cell Physiol* 2005;202:767-76.
10. Moessinger C, Kuerschner L, Spandl J, et al. Human lysophosphatidylcholine acyltransferases 1 and 2 are located in lipid droplets where they catalyze the formation of phosphatidylcholine. *J Biol Chem* 2011;286:21330-9.

Supplementary Figures

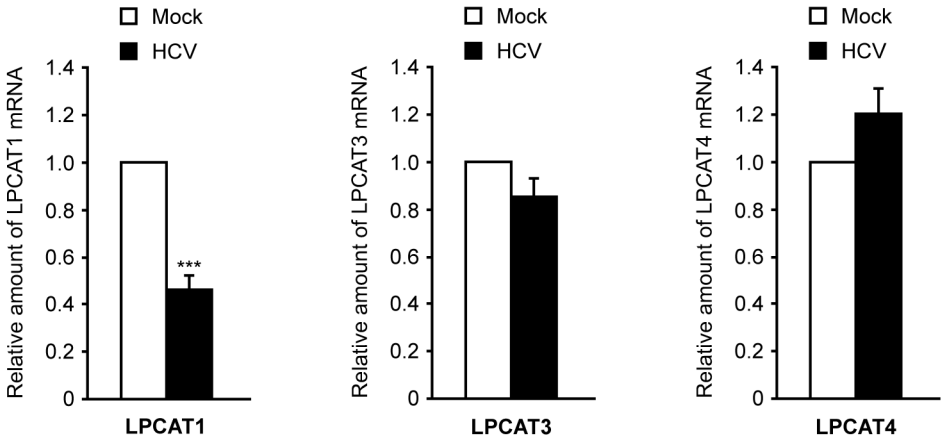

Figure S1. Effect of HCV infection on LPCAT expression. Huh-7.5.1 cells were inoculated or not with HCV, and lysed 3 days later for RT-qPCR analyses. Expression of the different LPCAT transcripts was normalised to that of human ribosomal protein L19 transcript. The means ± SEM of three independent experiments performed in triplicate are shown. Note that LPCAT2 was not expressed in these cells, as previously reported.[10]

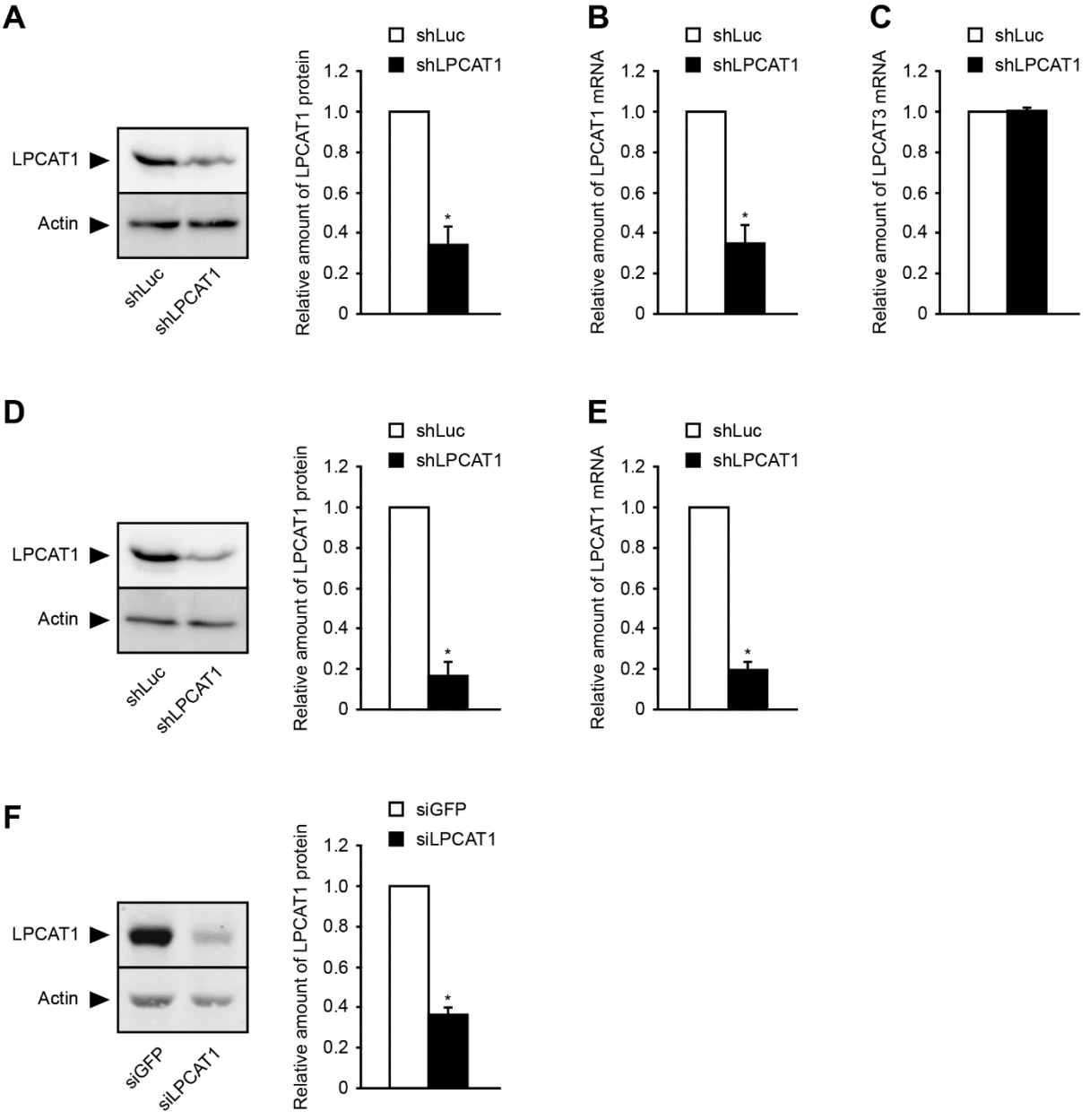

Figure S2. Efficiency of LPCAT1 silencing. (A-E) Huh-7.5.1 cells were transduced with lentiviral vectors encoding shLuc or shLPCAT1, and (A-C) left naïve or (D-E) inoculated with HCV 3 days later. (F) PHH were transfected with siGFP or siLPCAT1, and inoculated with HCV 3 days later. Three days post-inoculation, cells were lysed for (A, D and F) western blot and (B, C and E) RT-qPCR analyses. The means ± SEM of three independent experiments performed in triplicate are shown.

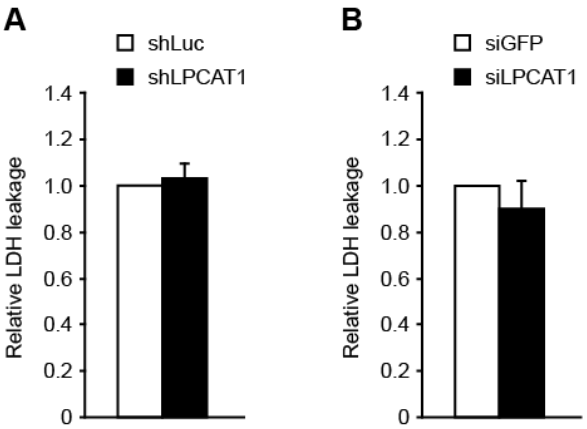

Figure S3. Absence of cytotoxicity upon LPCAT1 depletion. (A) Huh-7.5.1 cells were transduced with lentiviral vectors encoding shLuc or shLPCAT1, or (B) PHH were transfected with siGFP or siLPCAT1. Three days later, cells were inoculated with HCV, and culture supernatants were collected 3 days post-inoculation to measure lactate dehydrogenase (LDH) leakage. The means ± SEM of three independent experiments performed in triplicate are shown.

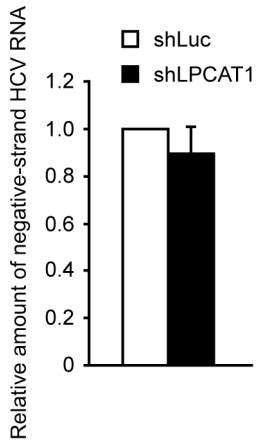

Figure S4. Absence of effect of LPCAT1 depletion on HCV genome replication. Huh-7.5.1 cells were transduced with lentiviral vectors encoding shLuc or shLPCAT1, and electroporated with HCV SGR 3 days later. Cells were lysed at day 1 post-electroporation for quantification of negative-strand HCV RNA. The means ± SEM of three independent experiments performed in triplicate are shown.

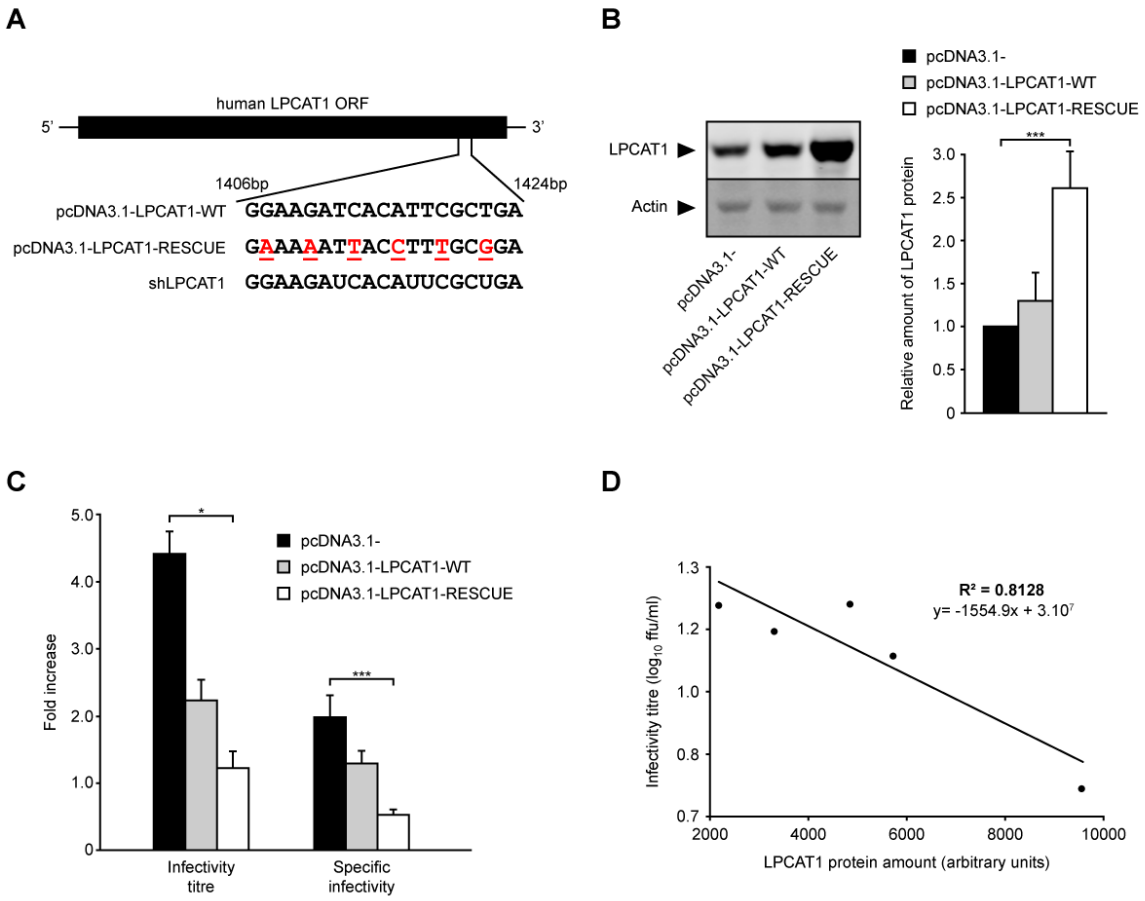

Figure S5. Effect of rescue of LPCAT1 expression in LPCAT1-depleted cells. (A) A mutant of LPCAT1 gene encoding a non-modified LPCAT1 protein but resistant to shLPCAT1 (RESCUE) was constructed. Shown are the sequences of shLPCAT1 and of the corresponding region in the plasmids carrying the wild-type (WT) or RESCUE version of LPCAT1 gene (pcDNA3.1-LPCAT1-WT and pcDNA3.1-LPCAT1-RESCUE, respectively). (B-D) Huh-7.5.1 cells were transduced with lentiviral vector encoding shLPCAT1, and inoculated with HCV 3 days later. The next day cells were transfected with empty plasmid pcDNA3.1- as control, or with pcDNA3.1-LPCAT1-WT or pcDNA3.1-LPCAT1-RESCUE, and cultured for 2 more days. (B) Cells were lysed for western blot analysis. (Left) A representative western blot is shown. (Right) LPCAT1 protein amounts were normalised to those of actin. The means ± SEM of three independent experiments performed in triplicate are shown. (C) Culture supernatants were collected for determination of infectivity titre and calculation of specific infectivity. Shown are the fold-increase values for shLPCAT1- compared to shLuc-transduced cells. The means ± SEM of three independent experiments performed in triplicate are shown. (D) Linear regression between LPCAT1 protein amount (as assessed by western blot quantification) and infectivity titre.